

REMARKS

Claims 1-87 were pending in this application prior to this Amendment. Claims 11, 12, 14, 15, 44, 59 and 84-87 are amended and claims 1-10, 21-43, 50, 62 and 75-82 have been canceled herein. Claims 88-130 are added herein.

Applicant would like to thank the Examiner for allowing claims 52-58, 68-74 and 83. Applicant also wishes to thank the Examiner for indicating the allowable subject matter of claims 16, 20, 50, 62, 63 and 65. As will be discussed below, the substance of each of these claims has been added to the now pending claims.

The Examiner has objected to the Information Disclosure Statement filed on December 11, 2000, for not including legible copies of two papers. Applicant has enclosed additional copies of these papers for the Examiner's convenience.

The Examiner has made numerous objections with respect to the drawings and the specification. Applicant has corrected each of these objections. Applicant respectfully submits that, to the best of Applicant's knowledge, the specification is now correct.

The Examiner has objected to claims 1, 11, 47, 75 and 87 for including informalities. For each of those claims that have not been canceled, these informalities have been corrected.

Claims 84-87 have been rejected under the second paragraph of §112. These claims have been amended to correct their dependency.

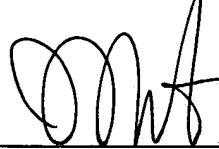
A number of the claims have been rejected in view of prior art. Each of these claims has either been cancelled herein, or amended to include subject matter of an allowable dependent claim. It is therefore respectfully submitted that each of the pending claims is now allowable.

Claims 88-130 have been added herein. It is respectfully submitted that each of these claims depends from a claim that has been indicated as being allowable by the Examiner. As per

claim 100, this claim includes the limitations of originally filed claim 20 and each of its intervening base claims. No new matter has been added.

In view of the above, Applicant respectfully requests that the present patent application be passed to issuance. No fee is believed due in connection with this filing. However, should one be deemed due, please charge Deposit Account No. 50-1065.

Respectfully submitted,



October 22, 2003

Date

Ira S. Matsil
Attorney for Applicants
Reg. No. 35,272

Slater & Matsil, L.L.P.
17950 Preston Rd., Suite 1000
Dallas, TX 75252-5793
Tel.: 972-732-1001
Fax: 972-732-9218

2/48

FIG. 1c
(PRIOR ART)

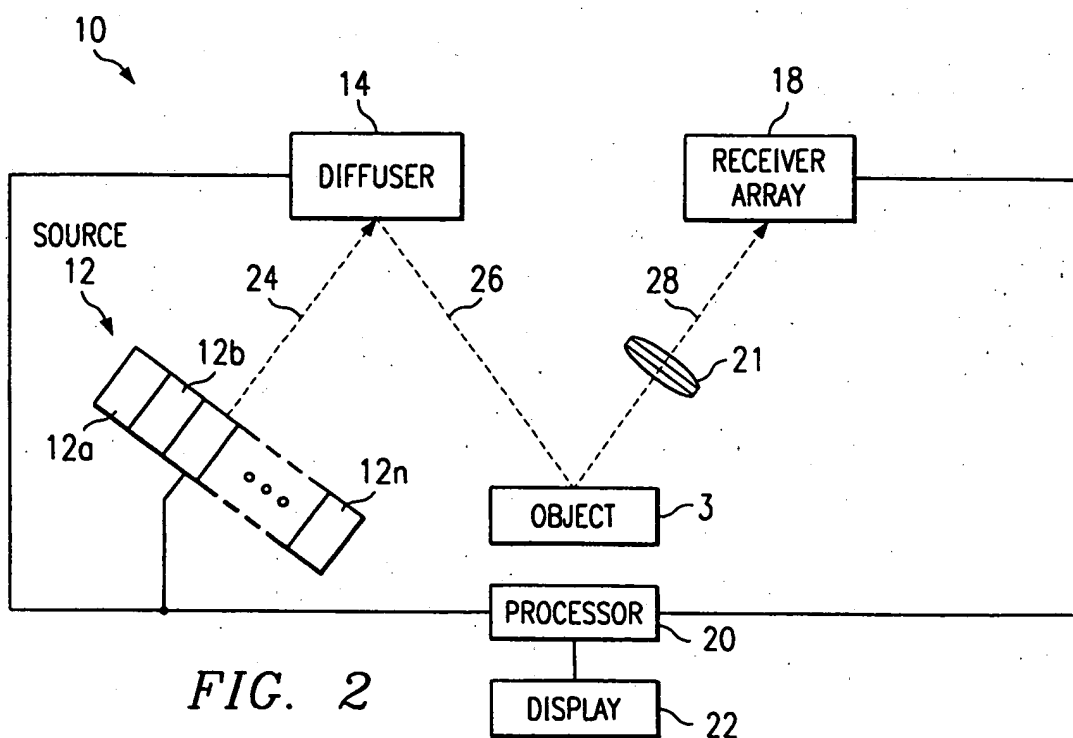
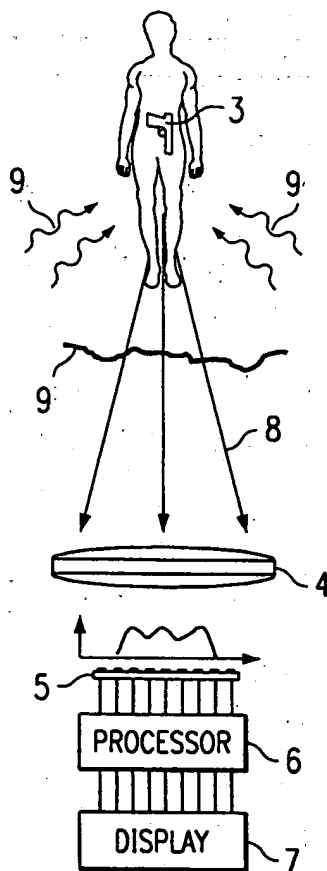
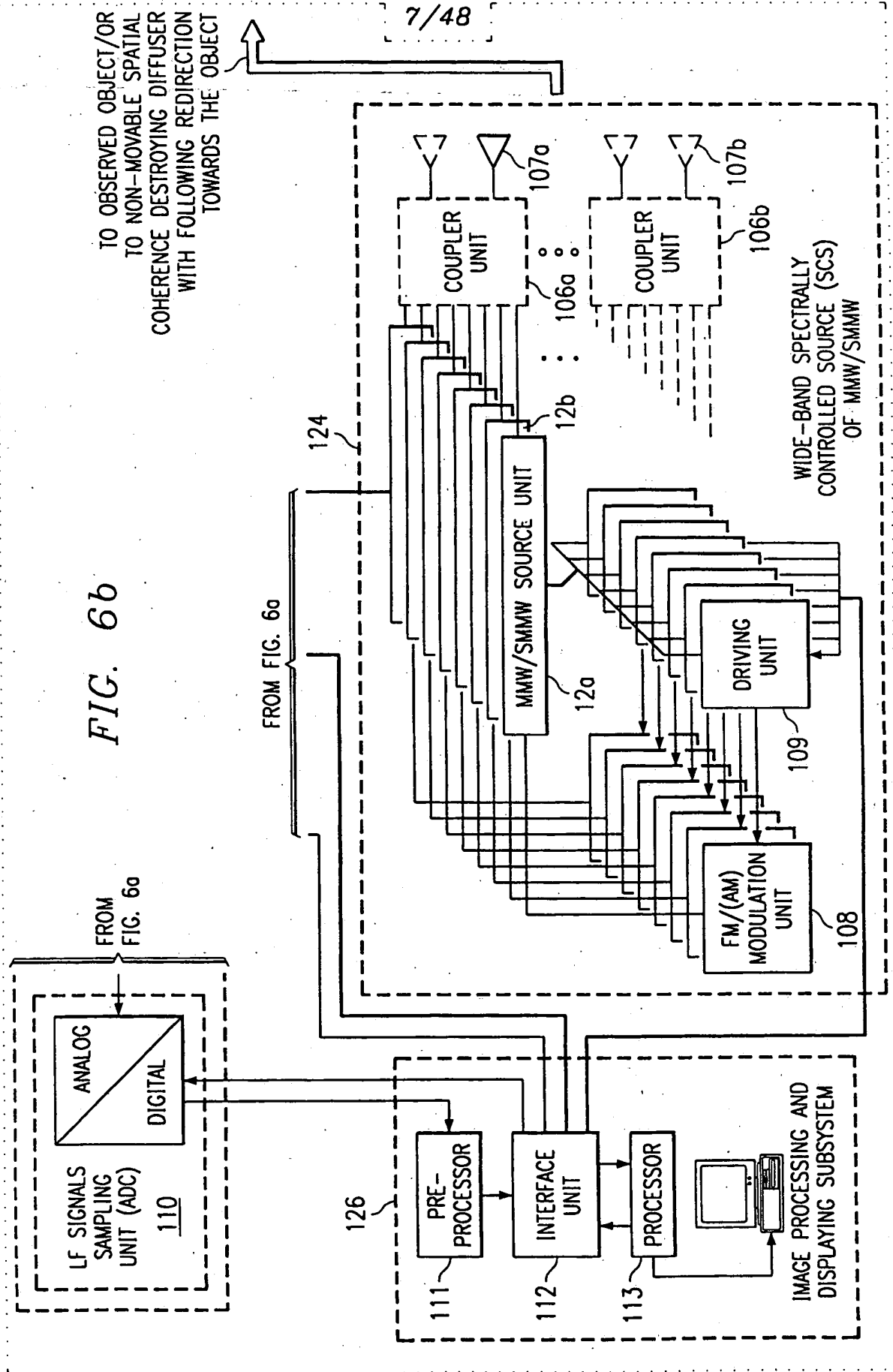


FIG. 6b





ROS8009

REPLACEMENT SHEET

9/48

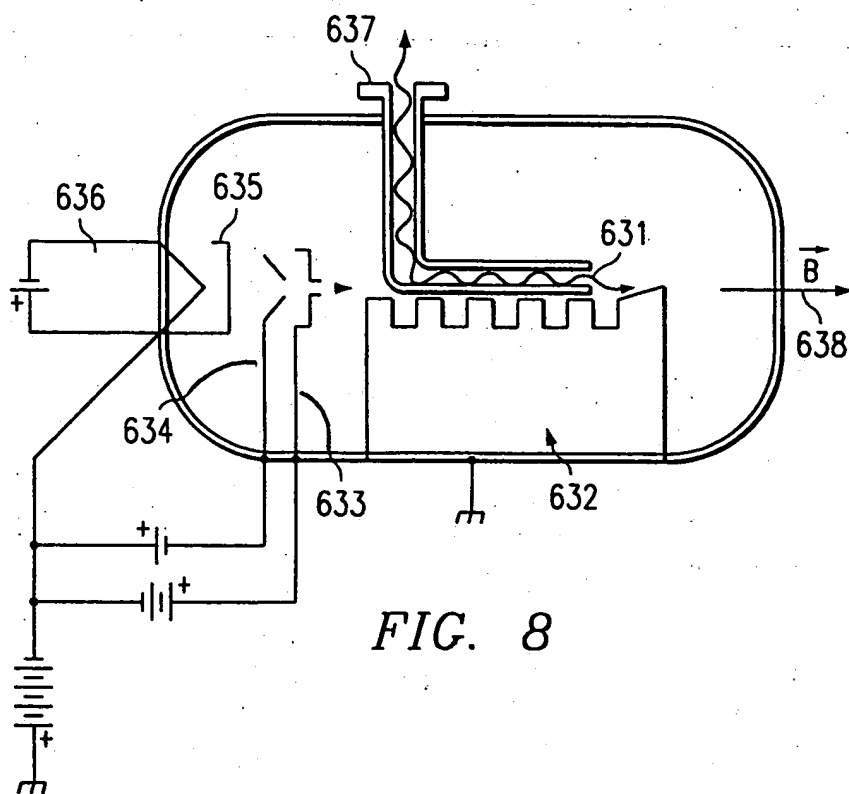


FIG. 8

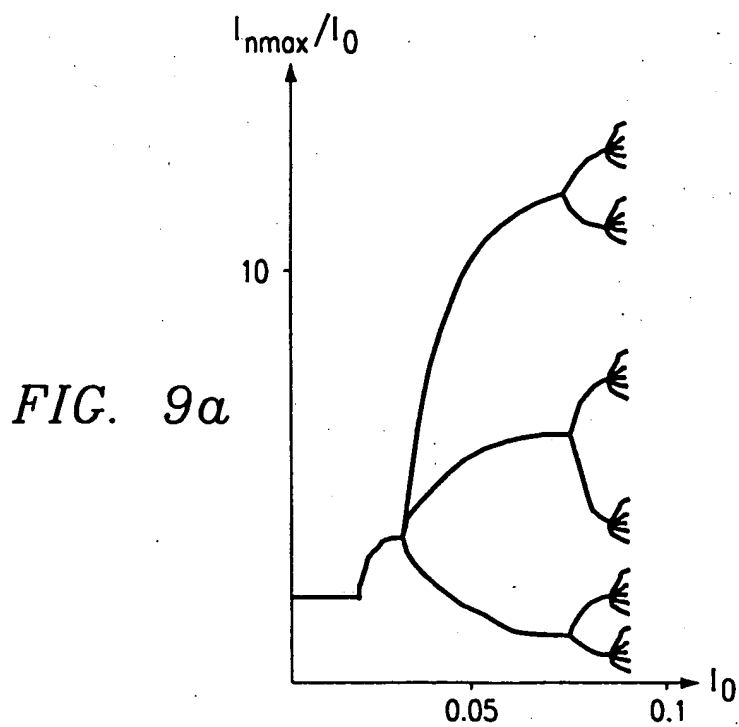


FIG. 9a



ROS8009

REPLACEMENT SHEET

11/48

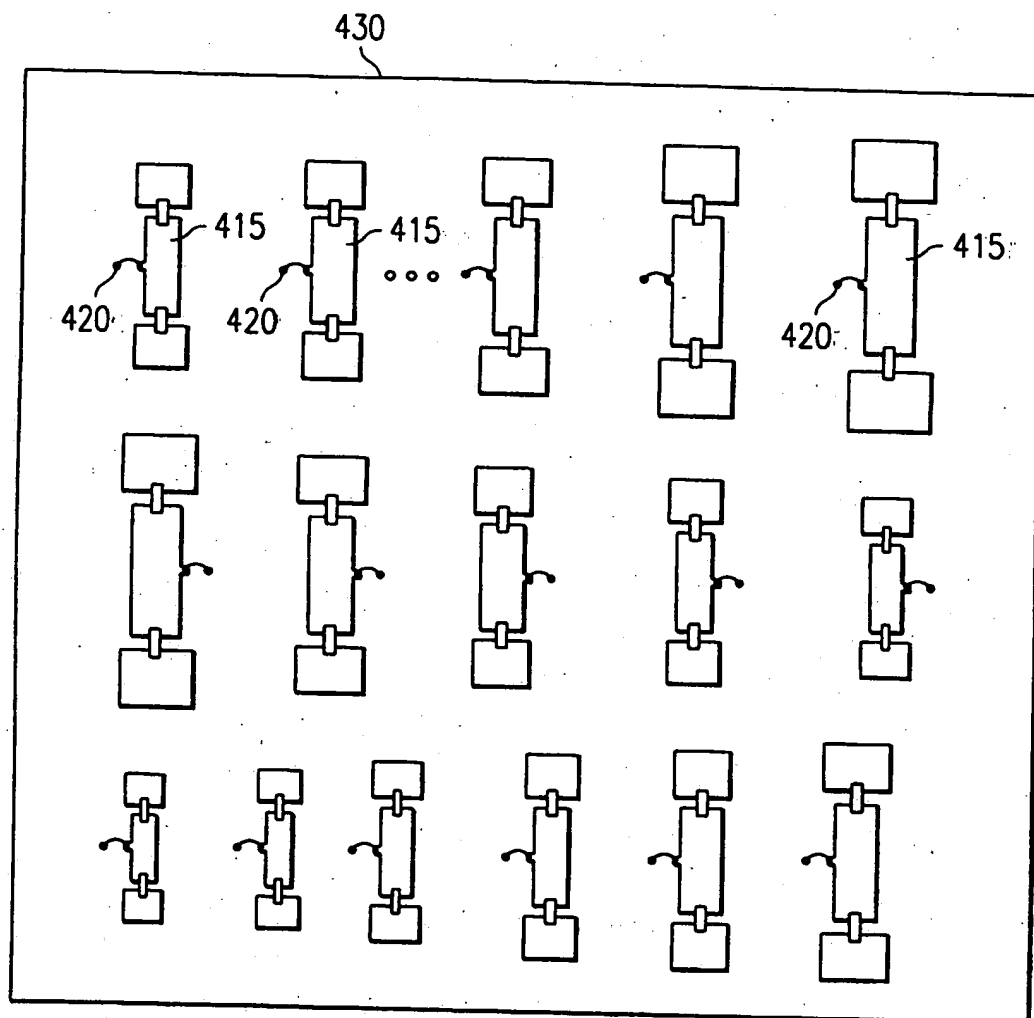


FIG. 11c



13/48

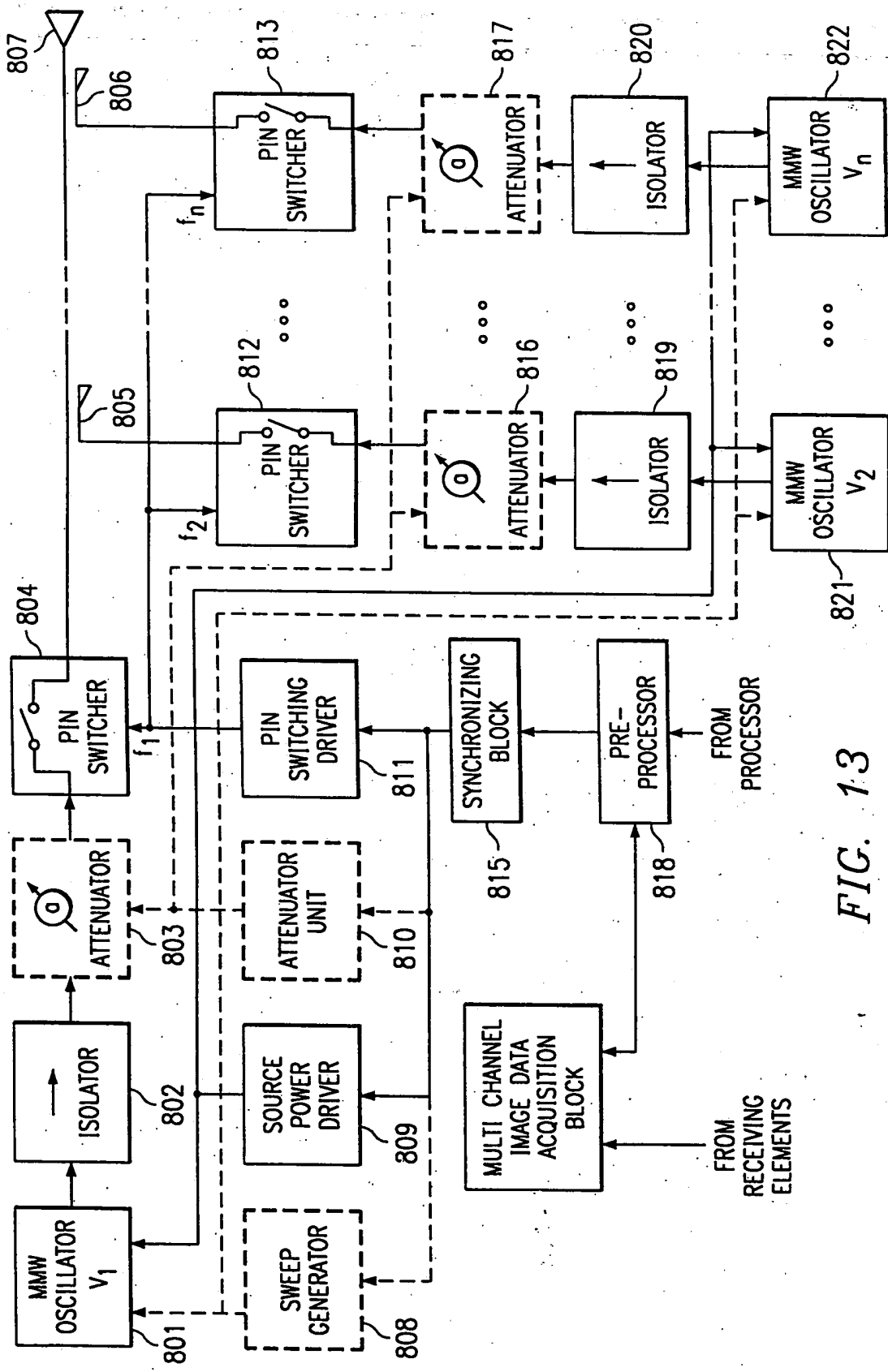


FIG. 13



ROS8009

REPLACEMENT SHEET

14/48

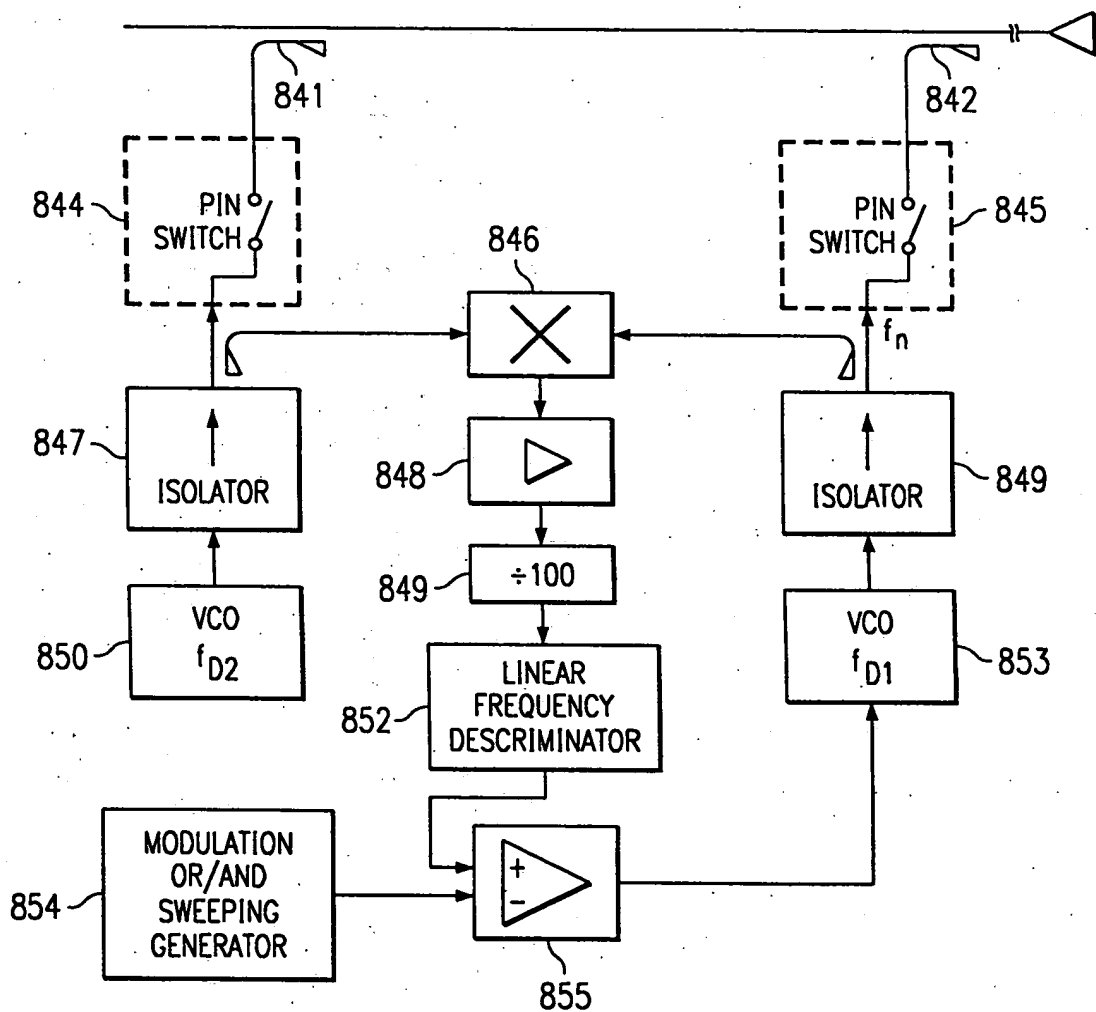


FIG. 14a



15/48

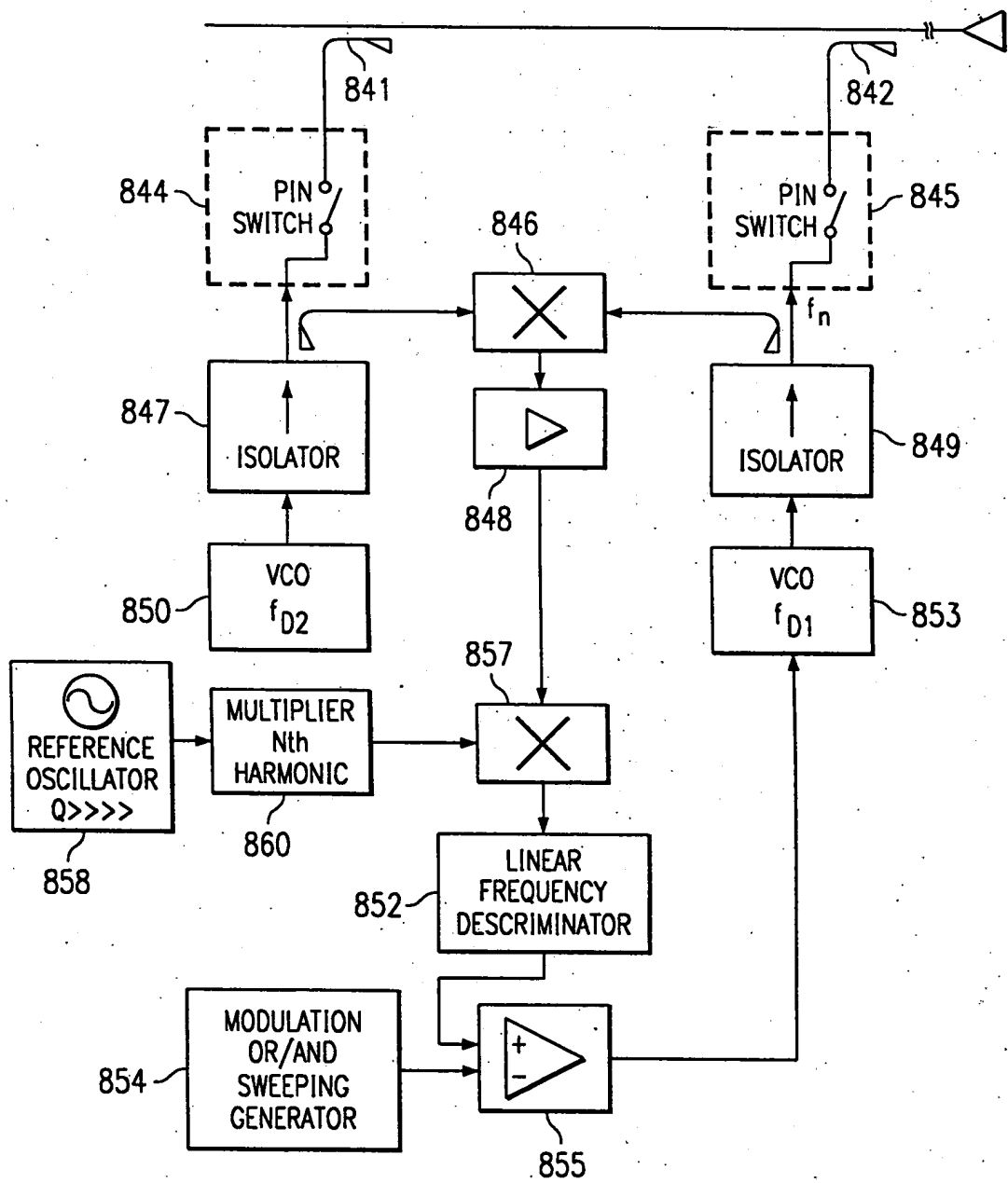


FIG. 14b

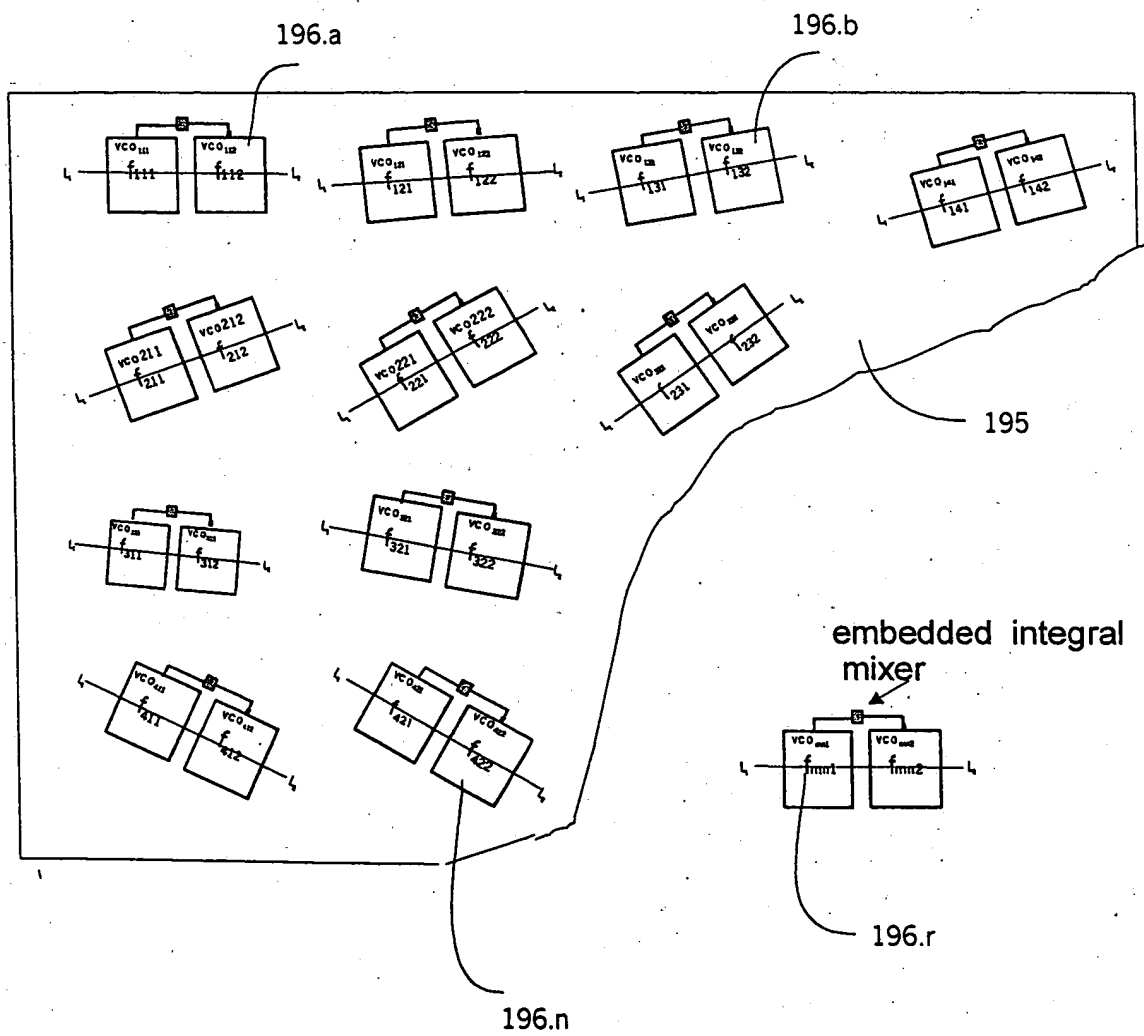


ROSE-8009

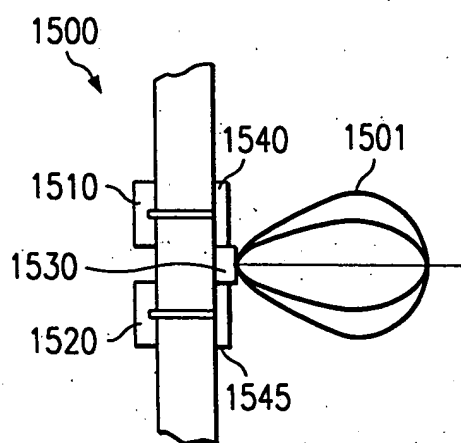
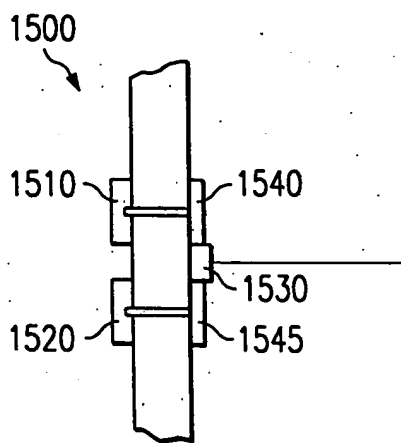
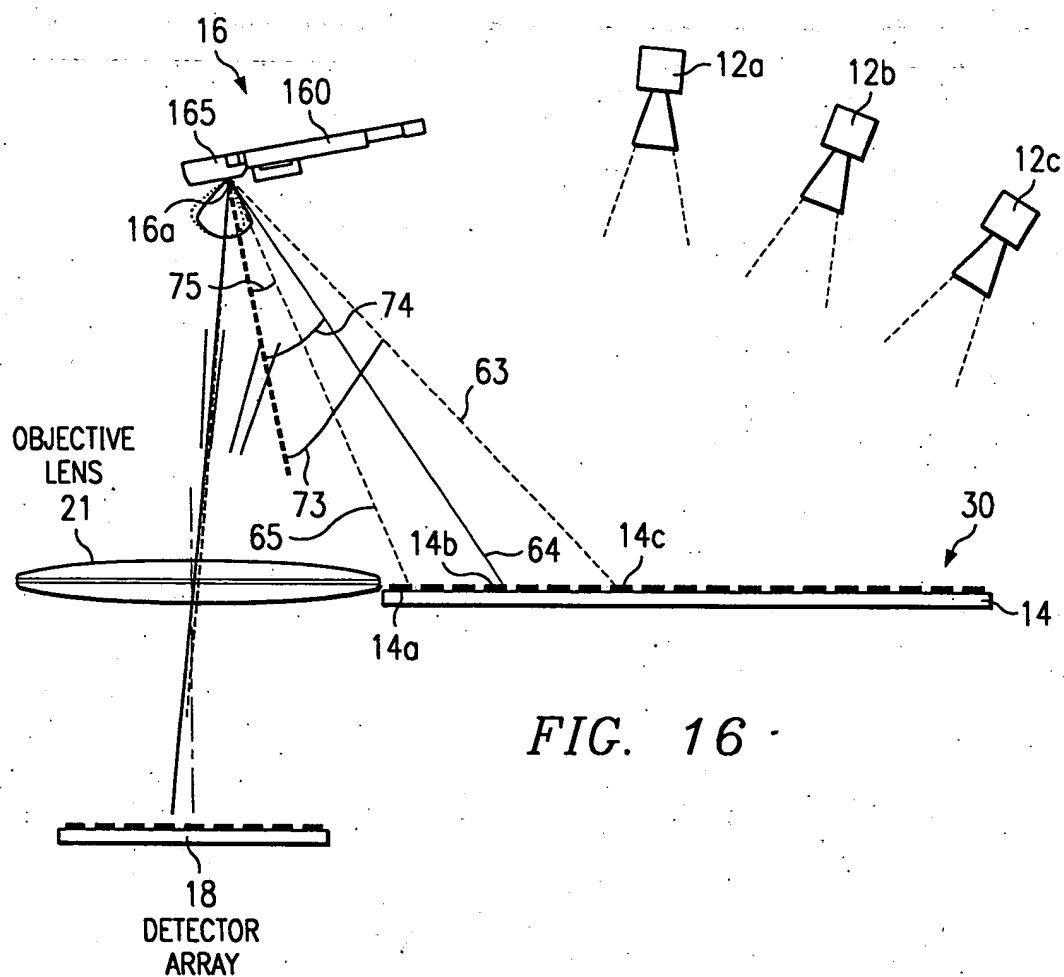
REPLACEMENT SHEET

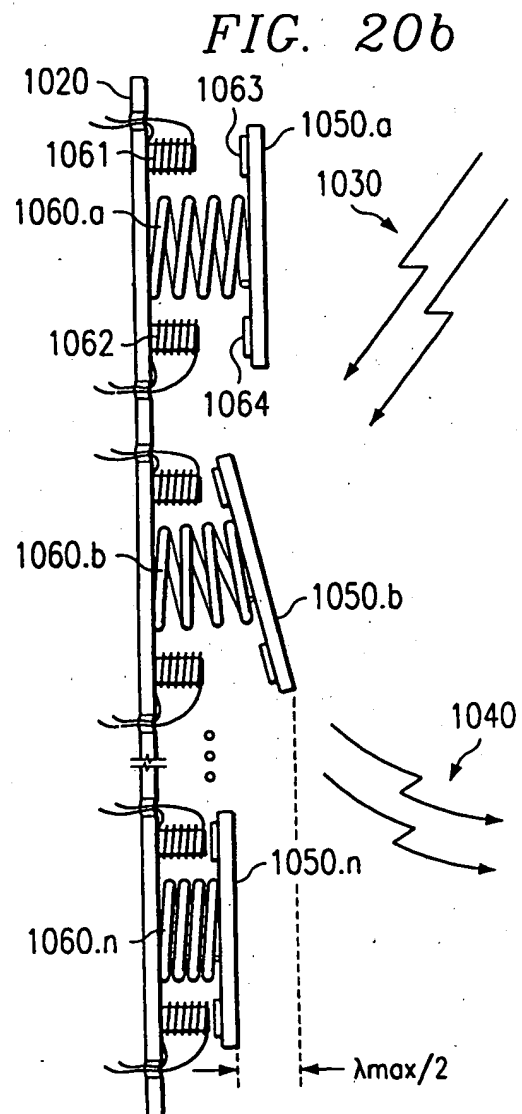
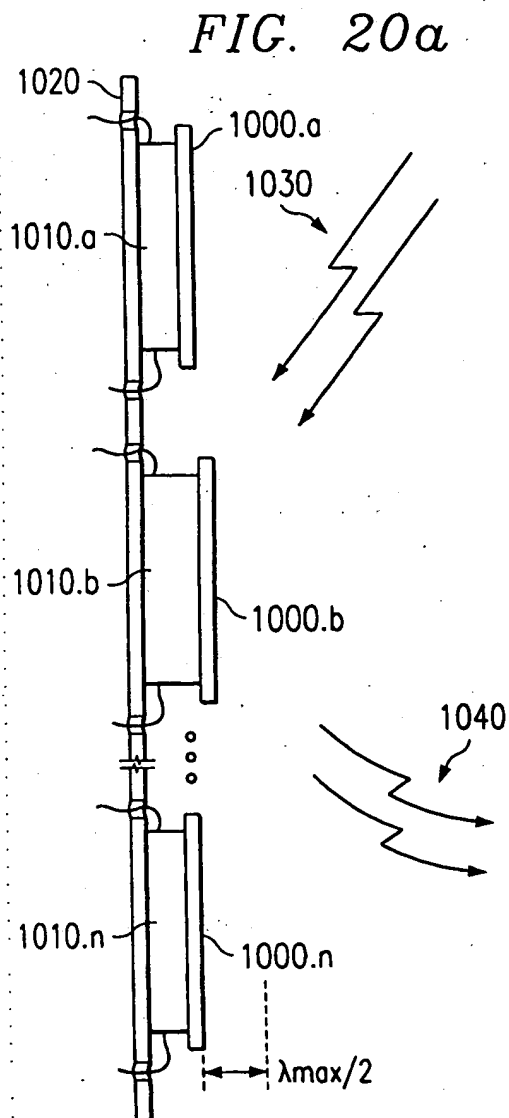
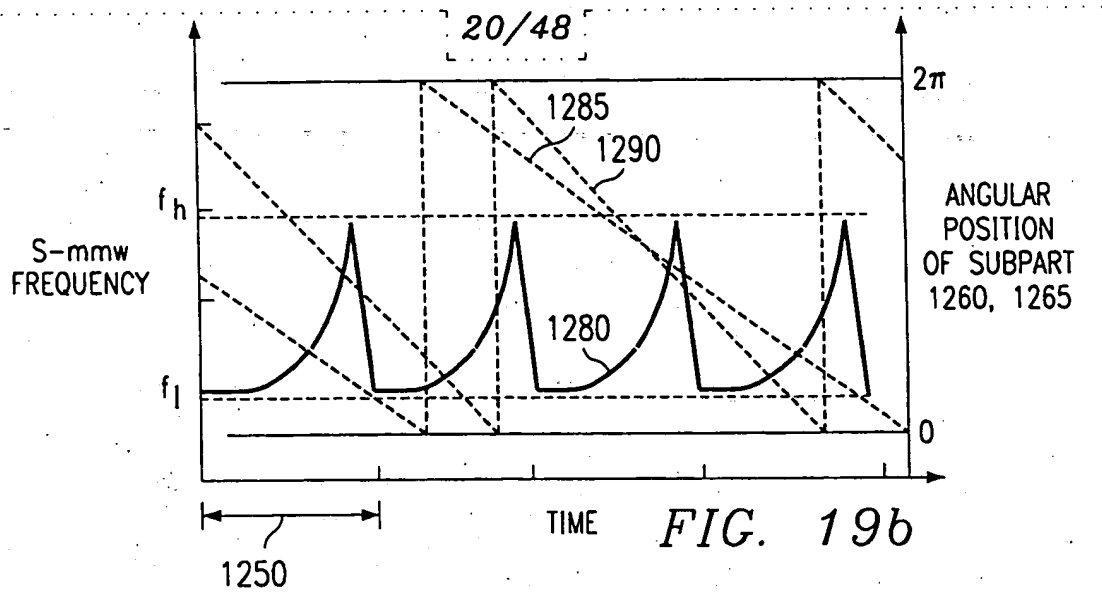
16/48

FIGURE 15



17/48





22/48

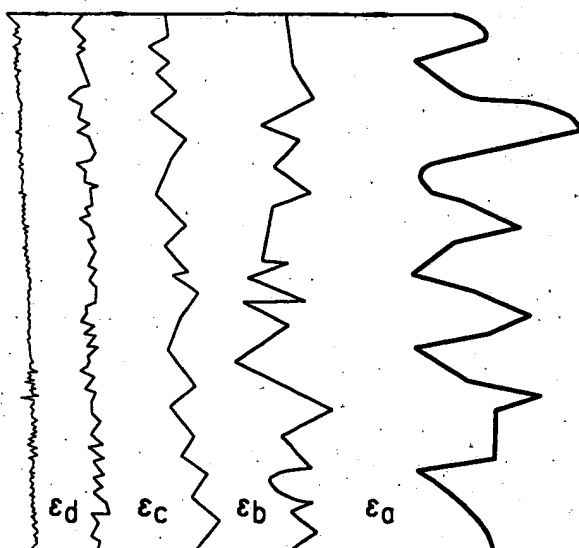


FIG. 23b

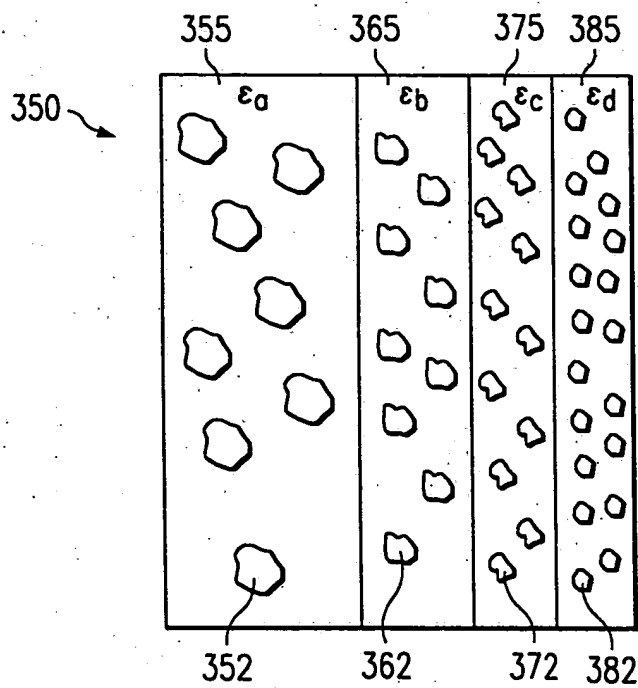


FIG. 24

27/48

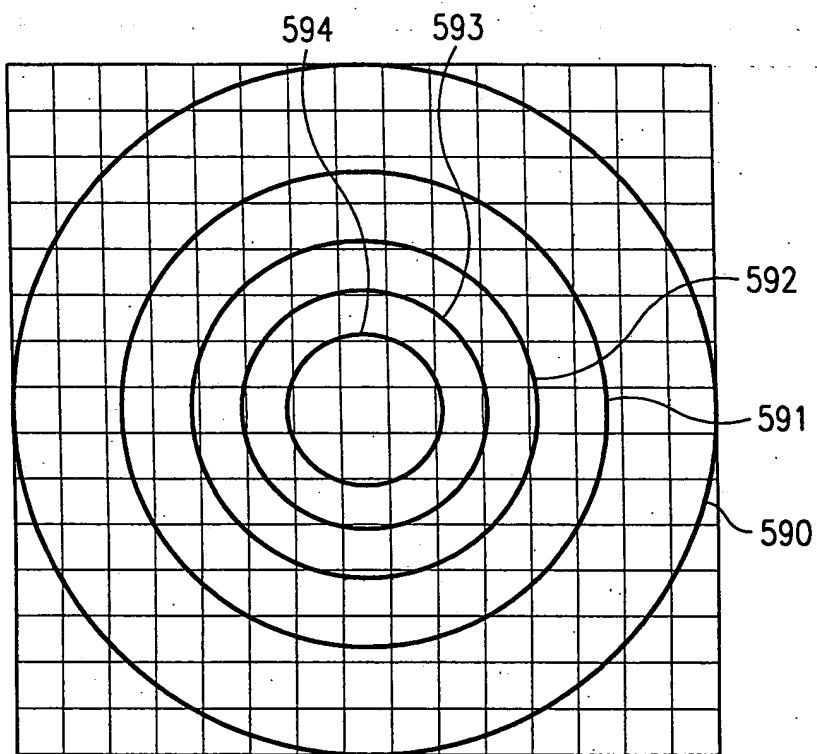


FIG. 29

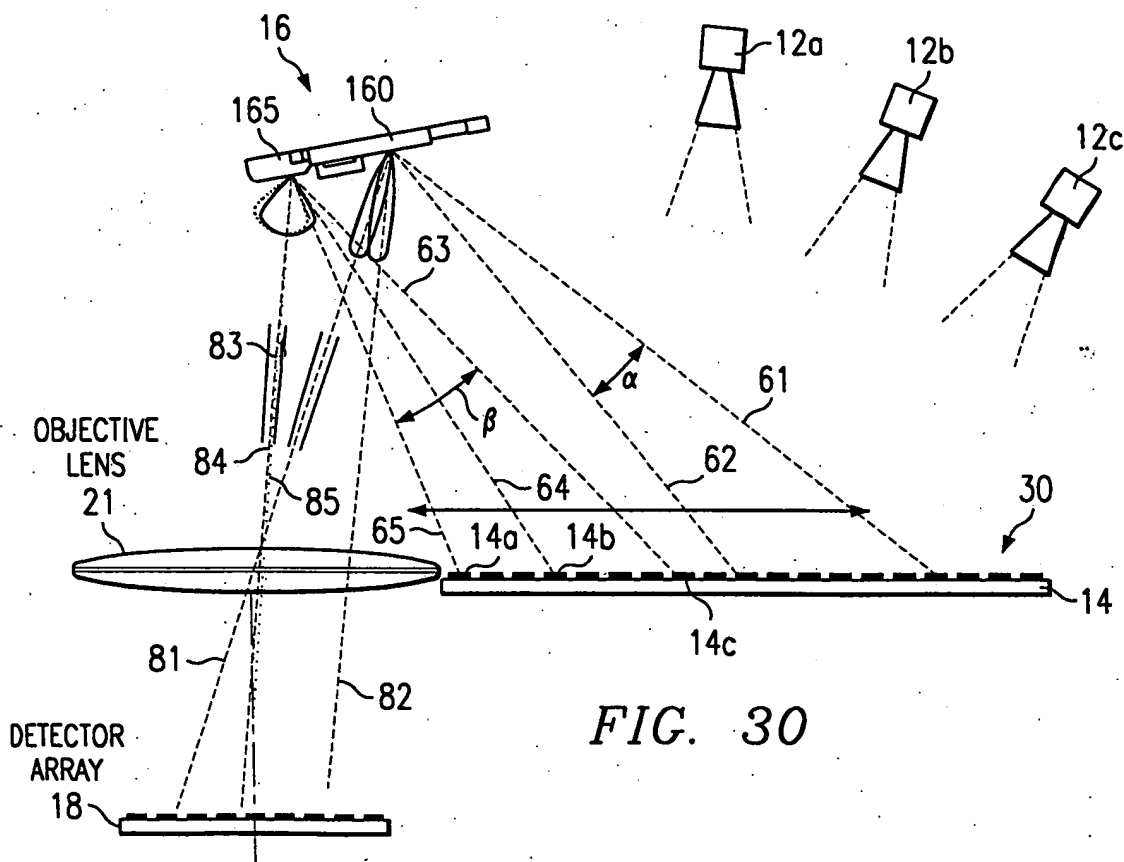
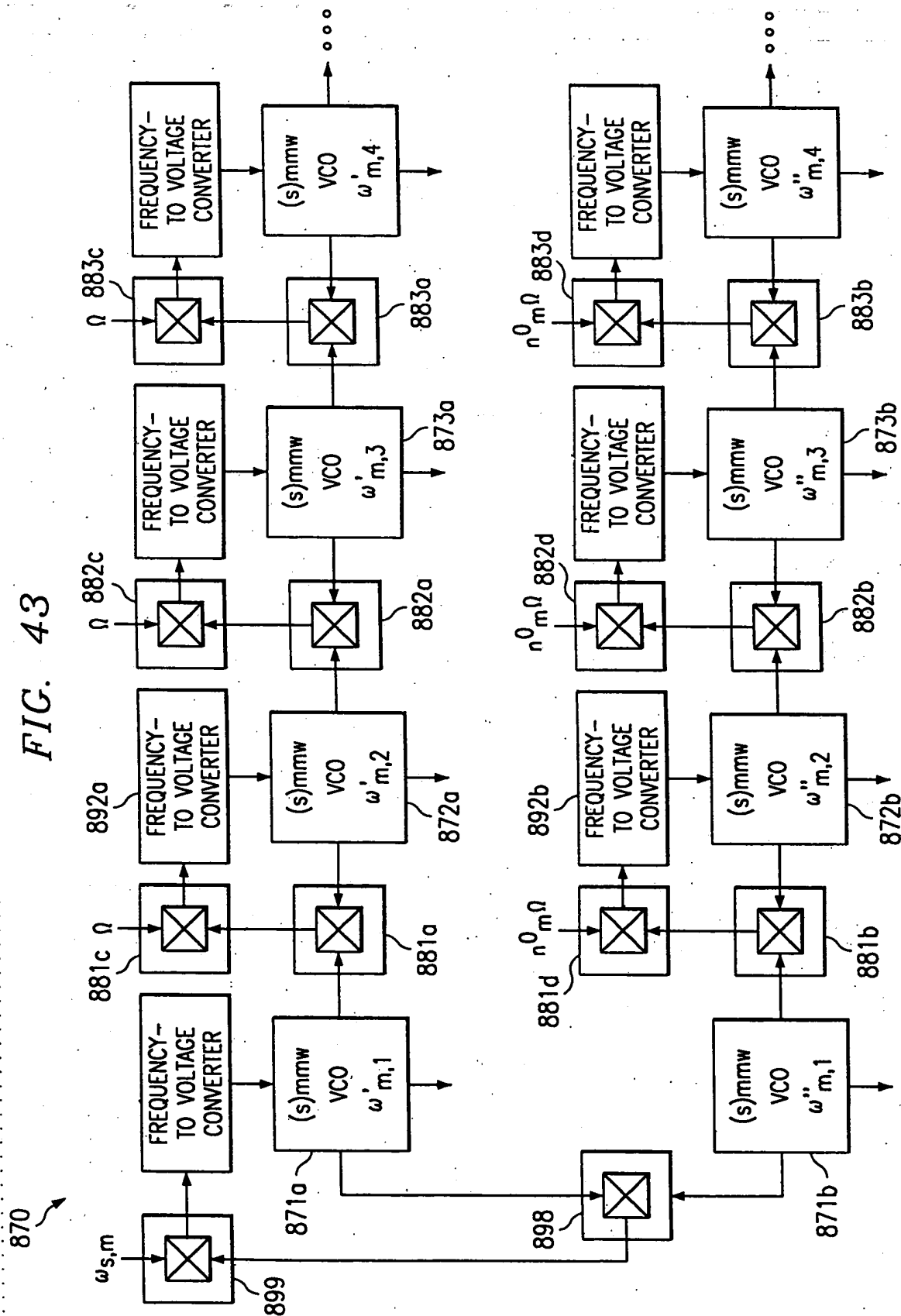


FIG. 30

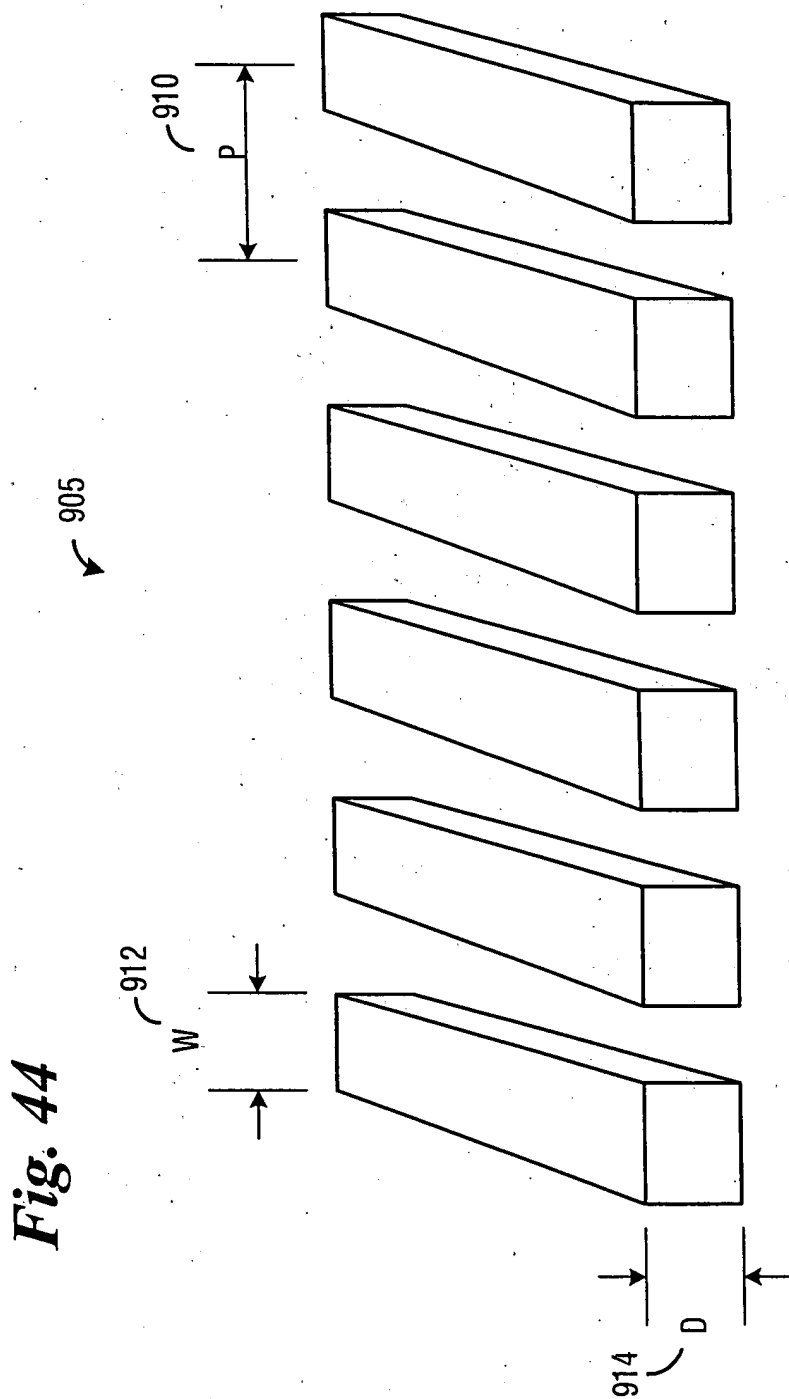
FIG. 43





ROSE-8009

38.1 / 48



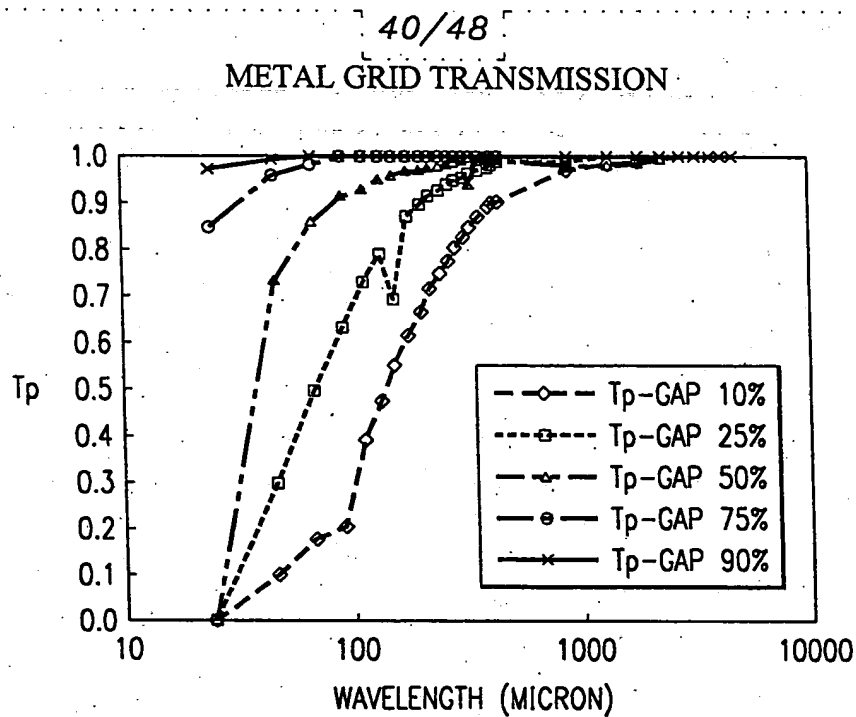


FIG. 46a

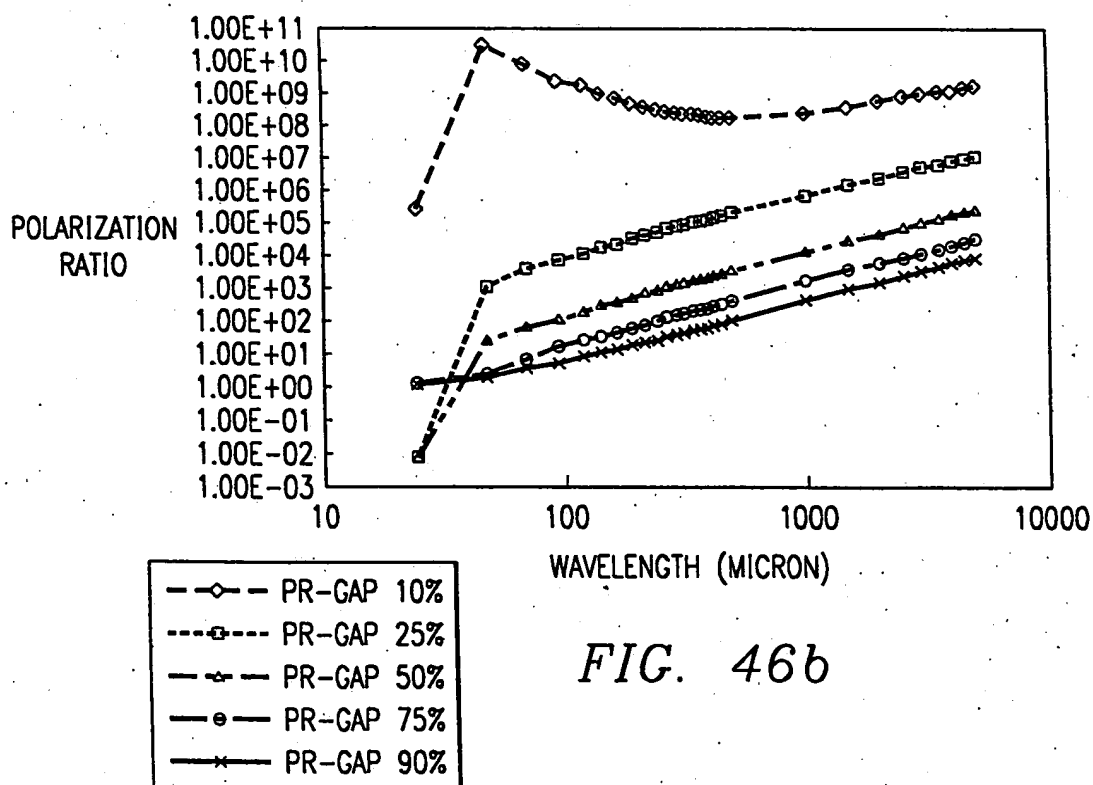


FIG. 46b

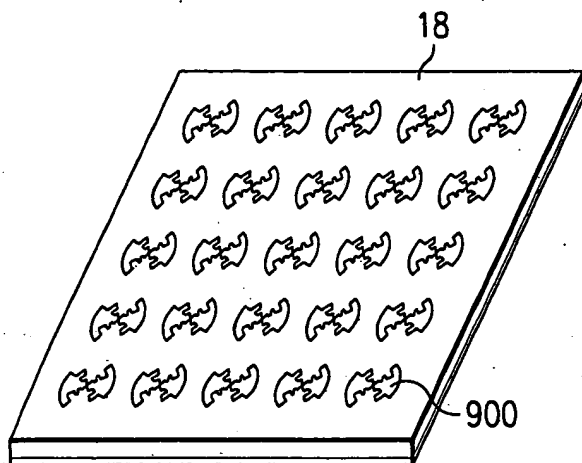
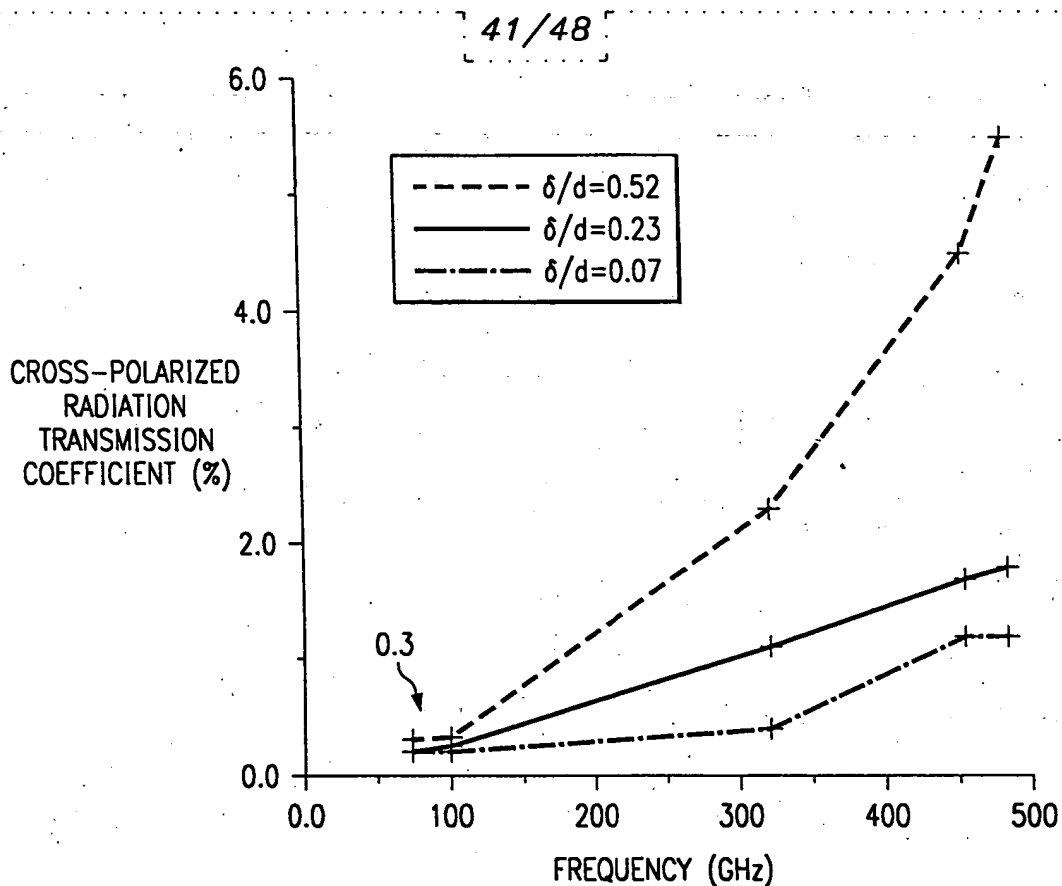


FIG. 48a

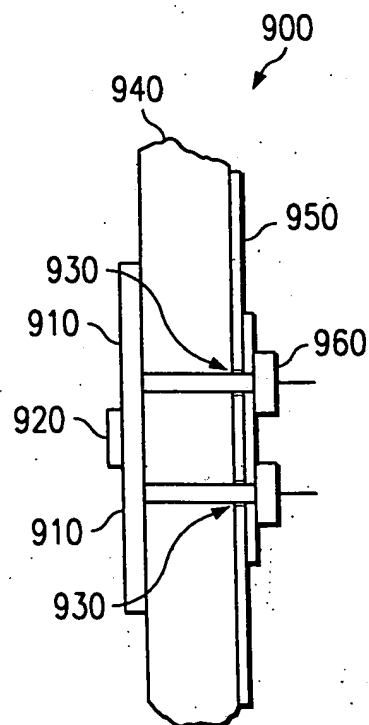


FIG. 48b

43/48

FIG. 50a

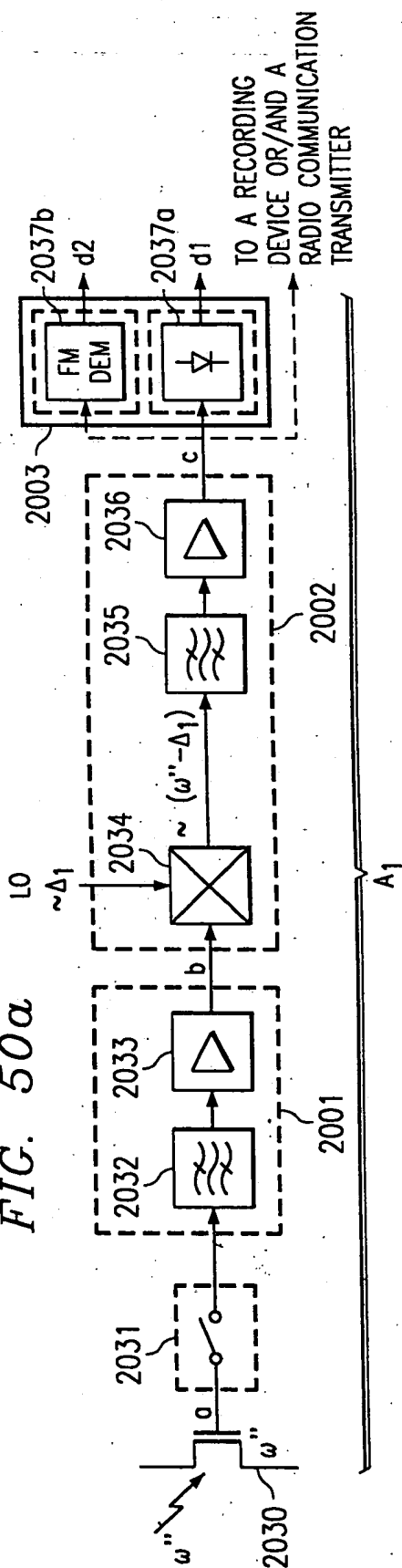


FIG. 50b

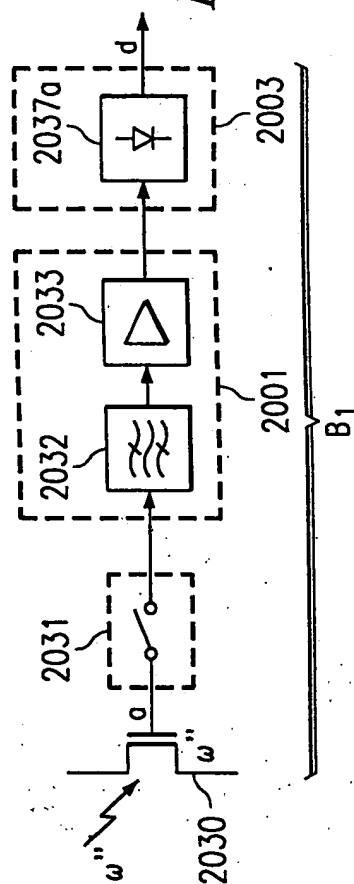


FIG. 50c

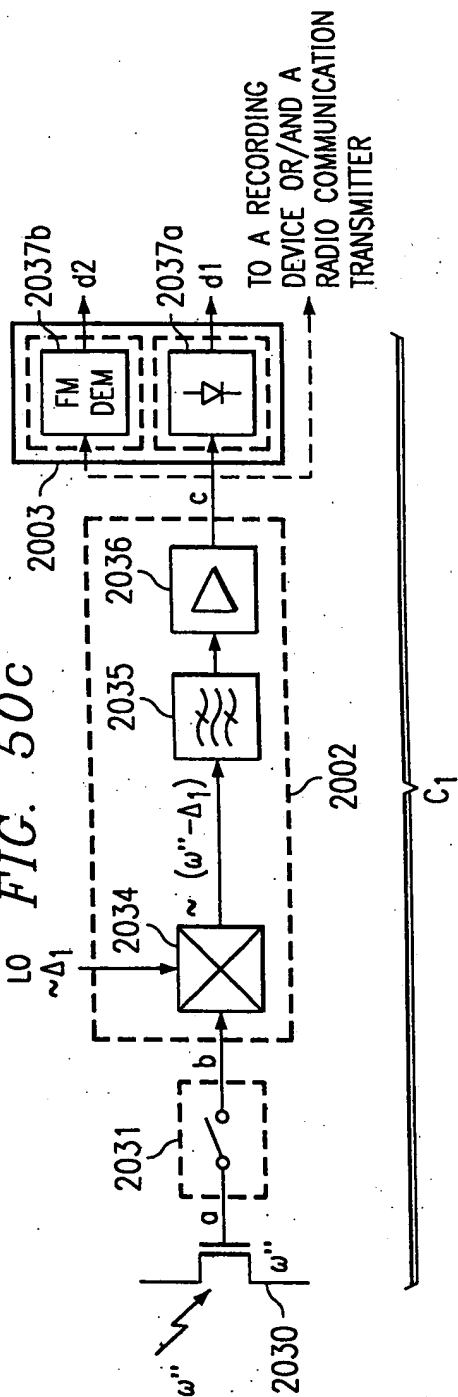
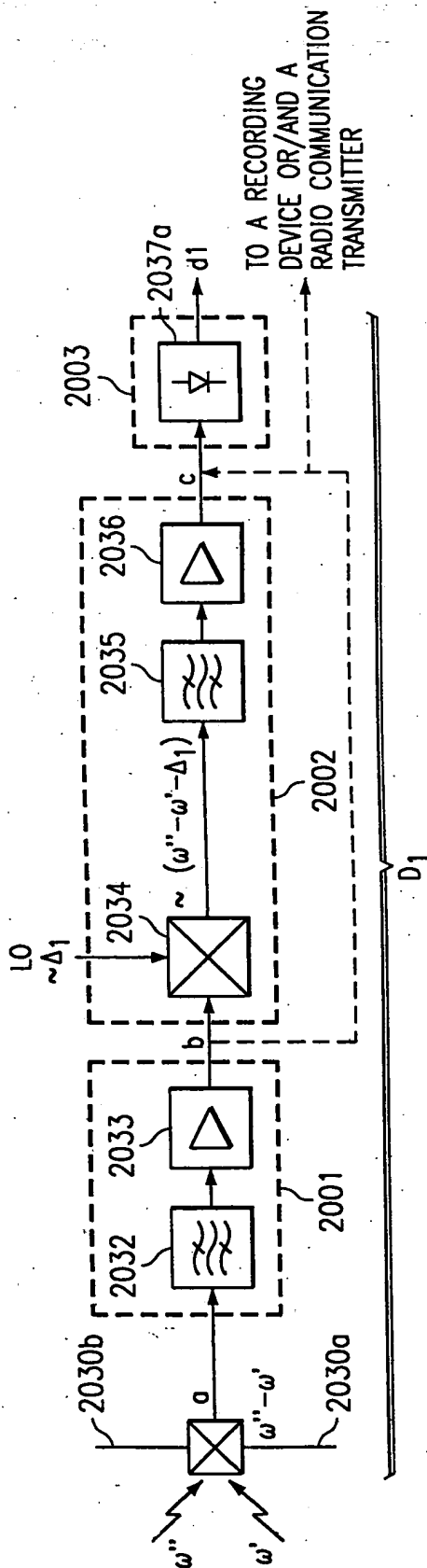
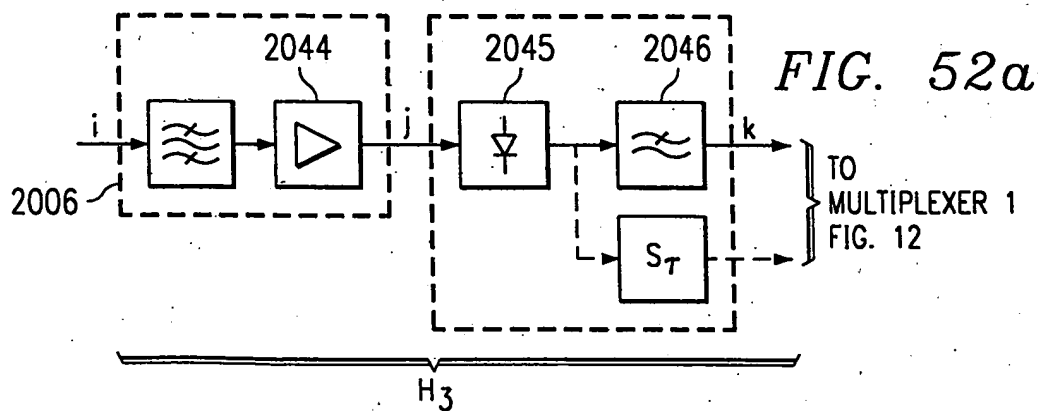
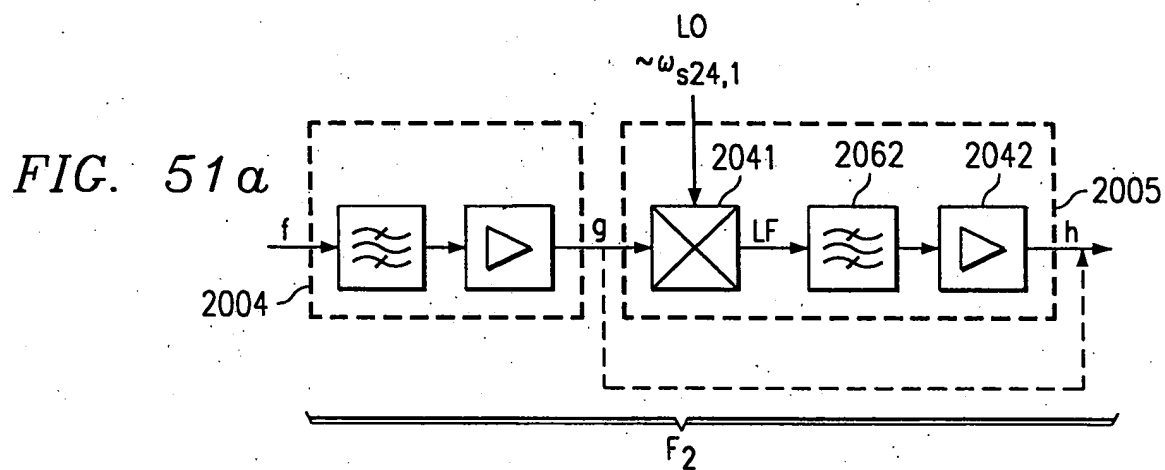
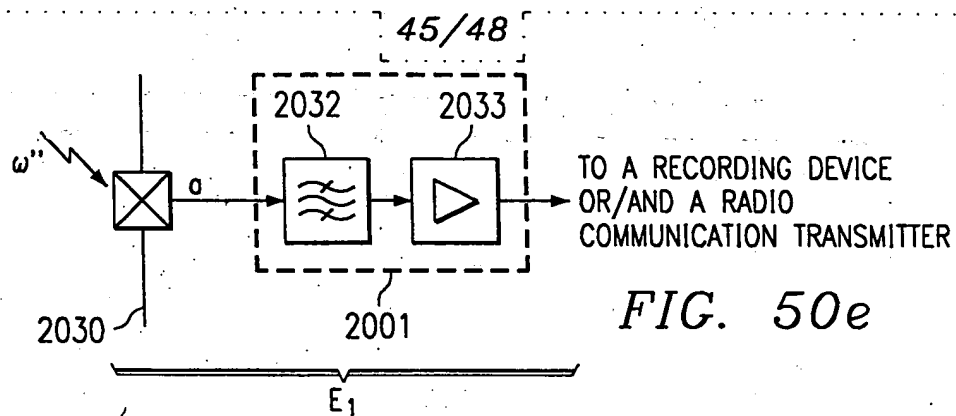


FIG. 50d





46/48

FIG. 52b

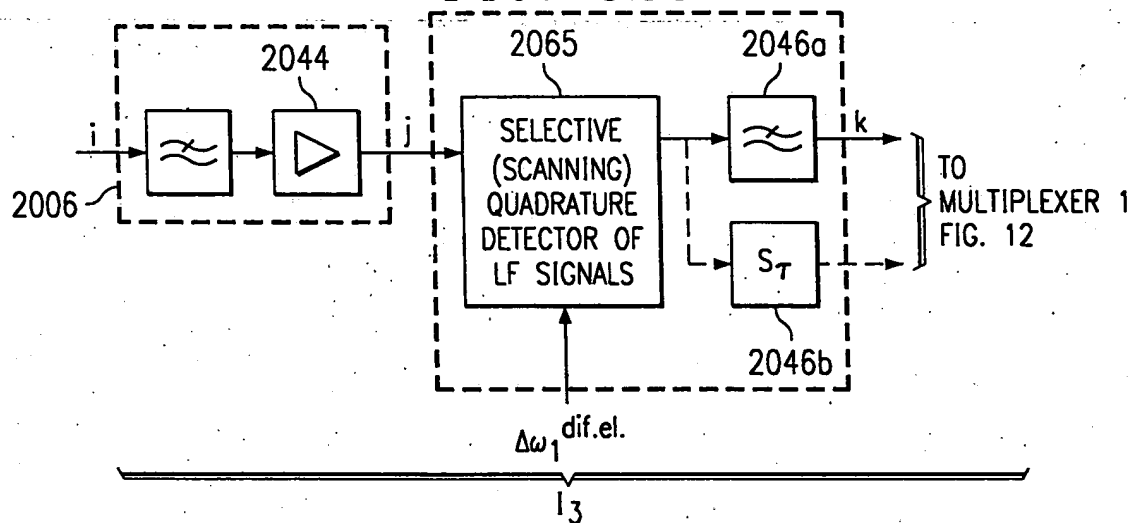


FIG. 52c

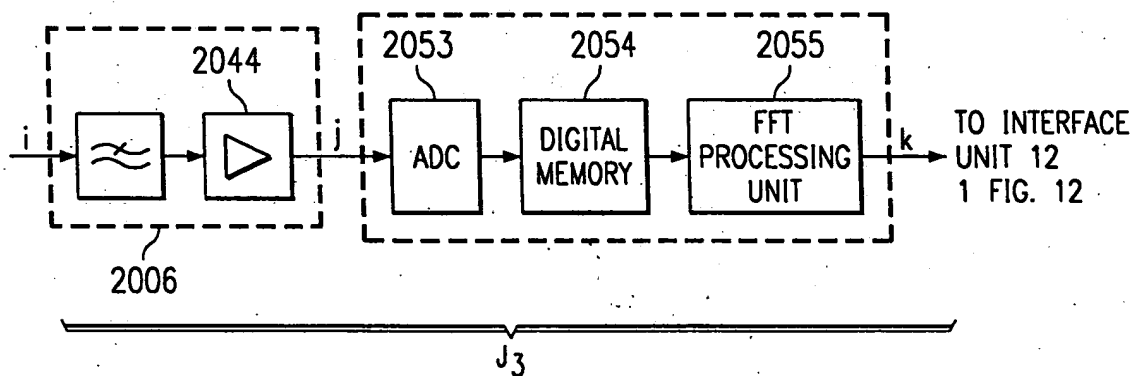


FIG. 53a

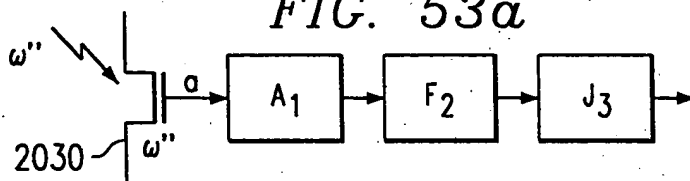
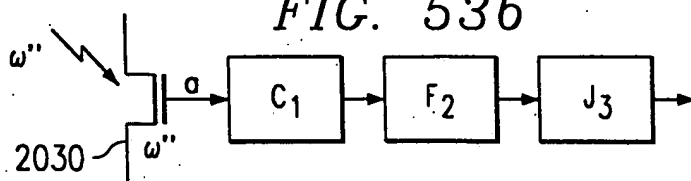


FIG. 53b



MILLIMETER WAVE IMAGING LENS ANTENNA

J. A. Clarke and R. J. Dewey

*Philips Research Laboratories
Redhill, Surrey, England*

Received October 3, 1983

The factors which influence the design of lenses suitable for imaging at millimetre wavelengths are discussed. Examples are given of optical designs for a military tracking application, firstly for use with an open ended waveguide array, and secondly for use with monolithic arrays, each covering a field of view of $\pm 20^\circ$.

Key words: millimetre wave imaging, optical design, arrays.

Introduction

In recent years the concepts of optical imaging have been applied in wavelength regions further and further from the visible range. Direct extensions of visible light techniques are sometimes possible, although radical changes may be necessary due to the limitations of materials and components at the desired wavelength. In the case of millimetre waves, however, the approach has often been more allied to microwave techniques, rather than optical techniques.

At the present time, most millimetre wave and far infrared imaging systems use a single detector and some form of mechanical scanning, rather than the more common visible technique of obtaining a complete picture at one time. In many cases the optics used are incapable of forming a good image of an extended scene - imaging is

obtained by mechanically directing the complete optical system at different parts of the object in sequence. Recent developments (1-4) have shown that arrays of detectors are now feasible and offer significant advantages in signal level, short picture acquisition time, and continuous monitoring of the whole scene. To take full advantage of the opportunities offered by arrays it is necessary to have optics with good imaging properties over a large field of view, and at the same time to match the optical design with the characteristics of the electronic components. In this paper we show how geometrical optics design principles have been used to design wide field imaging systems suitable for millimetre waves.

The optics described in this paper are for use at 90 GHz in a military tracking system. Lens optics are preferable to reflector optics as they are capable of covering a wider field of view and do not suffer from partial obscuration of the aperture, a feature of most reflector systems. One of the requirements is that the full diameter of the optics is used efficiently so that maximum signal is obtained in a physically limited space. Two applications will be considered. The first is for use with a matrix of open-ended waveguide elements, while the second is for use with monolithic arrays. First we must consider some optical principles which are common to both applications.

Optical Principles

The simplest lens system consists of just one component as shown in Fig. 1. We will consider the receiving mode although what follows is equally applicable to the transmitting mode. Radiation comes in from a distant target on the left, parallel to the lens axis, and the rays come to a focus on the right. If one of the lens surface is non-spherical, it is possible to obtain a perfect focus, limited only by diffraction effects.

Fig. 2 shows what happens if the radiation is not parallel to the axis. Upper and lower rays cross each other at one side of the central ray, an aberration known as coma. The best focus lies on a curved surface (field curvature). In addition, rays not in the plane of the diagram come to yet another focus (astigmatism), and the off-axis position is not linearly proportional to the input angle (distortion).

There is very little design freedom with only one lens and the only off-axis aberration that can be easily corrected is coma. This is done by shifting the power between the two surfaces. If the refractive index of the lens material is around 1.5, the optimum shape is near to plano-convex as in Fig. 2. Lenses which have very little coma approximately satisfy the Abbe Sine Condition (5). Such optical systems (often called aplanatic systems) are sometimes quoted as giving good performance over an extended field of view (6,7). When the field of view is $\pm 20^\circ$ or more, other off-axis aberrations such as field curvature and astigmatism predominate, and must be reduced to tolerable amounts.

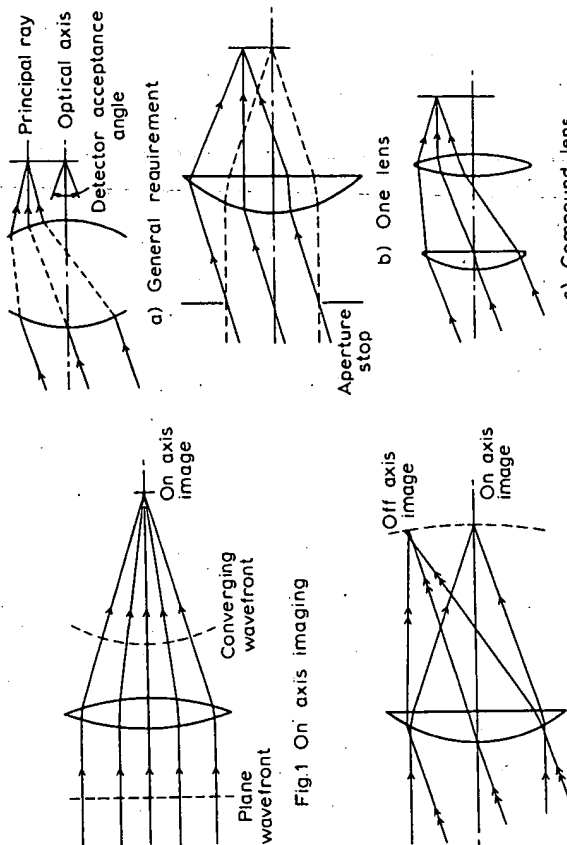


Fig. 1 On axis imaging

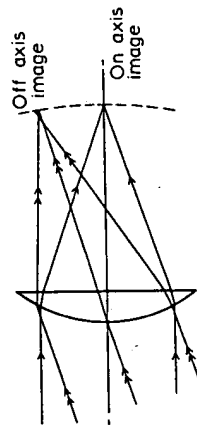


Fig. 2 Off axis imaging

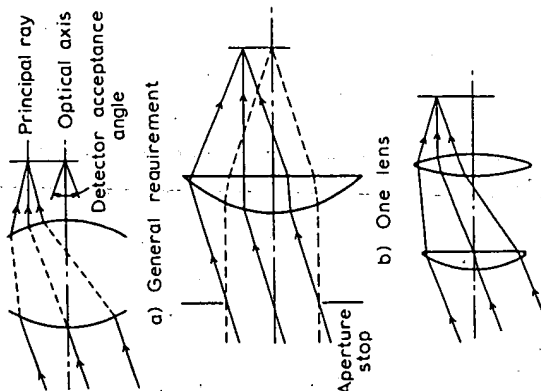


Fig. 3 Telecentric condition

So far the lens has been considered on its own. The image it forms must be detected, and the usual detectors (or transmitters) have their own constraints of physical size and directional properties. In particular, maximum signal is obtained if the radiation falls near the centre of the active area and within a given solid angle. If the aperture and focal length of the lens are chosen so that the on-axis image forming cone of rays matches the acceptance angle of the receiver, then loss of signal will result off-axis unless the off-axis cones of rays are also within the acceptance angle. In other words, the off-axis cones

which the lens will operate is known, diffraction effects will determine the far-field resolution for a given diameter lens. In our case the diameter is limited to 80 mm for mechanical reasons, resulting in a resolution of 2.5° . The useful acceptance angle of the receiver is $\pm 45^\circ$, so this fixes the optimum aperture ratio of the lens at F/0.7. The aperture ratio and diameter fix the focal length at 57 mm. Lastly we set ourselves the target of $\pm 20^\circ$ field of view, giving 16 picture elements across the image.

Lens for Open-Ended Waveguides

The foregoing concepts can be used to design the lens for the open-ended waveguide application. The 2-element lens shown in Fig. 3c will satisfy the telecentric condition, but as both components are positive lenses, they will not give a flat image. A negative lens is also needed and this can be placed near the image as shown in Fig. 4. The resulting design, when optimised, easily satisfies all of the requirements set out in the specification, and could be used with a field of view of $\pm 23^\circ$.

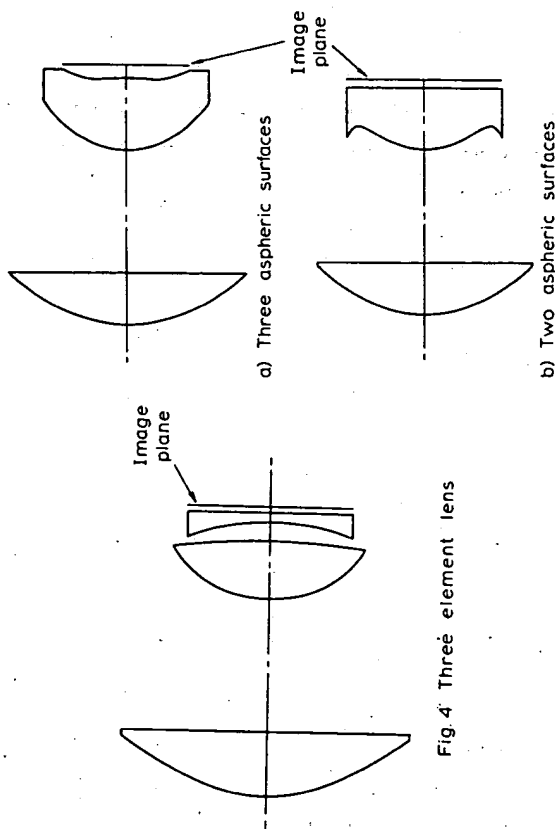


Fig. 4 Three element lens

a) Three aspheric surfaces

b) Two aspheric surfaces

Fig. 5 Two element lenses

must not be tilted over as in Fig. 2. What is needed is an arrangement where the central (or principal) ray of each off-axis cone is parallel to the axis as in Fig. 3a. It is only possible to achieve this condition (known as a telecentric pupil) with a single thin lens if a limiting aperture is placed some distance in front of the lens, and the lens itself is made substantially larger than necessary for the on-axis rays as shown in Fig. 3b. This does not make very efficient use of a physically restricted aperture. The use of a compound lens with two or more components enables the telecentric pupil condition to be met without making the lens oversize (Fig. 3c). The extra lens surfaces also provide additional degrees of freedom to correct some of the remaining off-axis aberrations.

The problem of absorption in the lens material becomes more important if there are several lenses. For refracting lenses there is the requirement that the material must be non-absorbing in thicknesses of about 25 mm, and also obtainable at reasonable cost in diameters up to about 100 mm. Table I shows some possible materials (8). At the top are a number of plastics, followed by natural materials - quartz, silicon, and germanium, and lastly the Stycast range, not all of which are suitable at 90 GHz. Rexolite 1422 has very good mechanical properties, and a slightly higher refractive index than the other plastics. As we had had previous experience of this material, it was chosen for the open-ended horn application.

MATERIAL	DIELECTRIC CONSTANT	REFRACTIVE INDEX
"Teflon"	2.06	1.44
Polyolefine, "TPX"	2.12	1.46
Polyethylene	2.25	1.52
Cross linked Polystyrene	2.53	1.59
"Rexolite"		
Fused quartz	3.81	1.95
Silicon	11.6	3.40
Germanium	16.0	4.00
"Stycast HiK"	3.0 - 30.0	1.73 - 5.5

Table I: Materials for Millimetre Wave Lenses

Having decided on the material for the lens, it is still necessary to agree on a number of other parameters before detailed design can begin. If the frequency or wavelength at

Examination of this design shows that the 2nd and 3rd elements are close together, so a logical step would be to combine them into one thick lens, with the first surface satisfying the telecentric condition and the other surface providing the flat field as shown in Fig. 5a. The wavefront errors of this design are less than 0.03 wavelengths, except near the extreme field angle of 20°, where there is just less than 0.1 wavelength of astigmatism and coma. Although the theoretical performance is well within the specification the second element would be difficult to manufacture as it has an aspheric surface on both sides, and these would have to be accurately centred with respect to each other.

At 3 mm wavelength diffraction effects predominate so the aberrations could be much larger - up to 0.25 wavelength. Alternative designs in which only one surface of each lens was aspheric were therefore considered. It was found that a 2-element design satisfying this restriction but with adequate performance could be realised, as shown in Fig. 5b. The second element of this has a highly aspheric profile which is convex in the centre, but becomes concave towards the edge. In this design, not only do both elements have only one aspheric surface, but they are also flat on the other side making for ease of manufacture. The theoretical wavefront error on-axis is less than 0.005 wavelength. Off-axis astigmatism and coma reach a maximum of 0.18 wavelength at about 17°, then a slight decrease out to 20°.

A numerically controlled lathe was used to make a lens to this design. The far-field radiation pattern of the assembled lens was measured using a single horn feed. This was moved to various off-axis positions at 4 mm intervals. Fig. 6 shows the signal level in dB plotted on a polar diagram. Out to $\pm 16^\circ$ the performance is very uniform, being limited mainly by diffraction, while at $\pm 20^\circ$ there is a small loss of signal (about 3 dB) due to vignetting of the extreme rays and a small geometrical aberration contribution. This loss of signal is shown, together with the geometrical distortion, in Fig. 7.

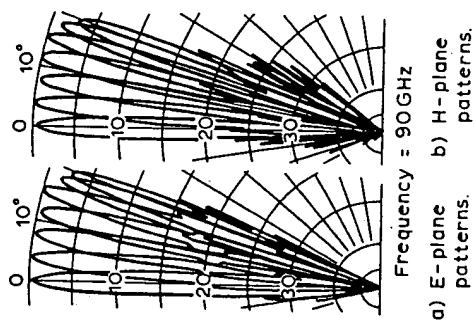


Fig. 6 Radiation patterns for dual-lens antenna

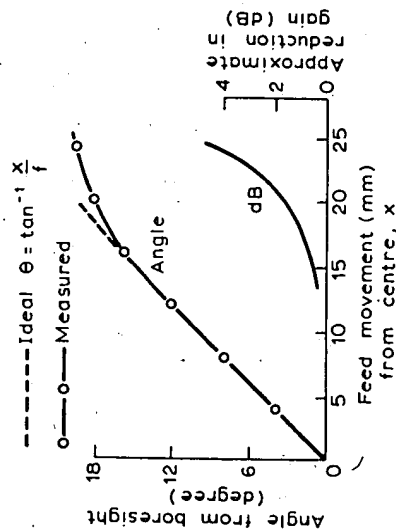


Fig. 7 Variation of scan angle and gain degradation with feed position in dual-lens antenna.

Lens for Monolithic Array

The future for millimetre wave imaging depends on the progress obtained with fabricating and using monolithic arrays instead of open horn feeds. Monolithic construction would enable the array elements, mixers, and amplifiers to be fabricated on a single semiconductor substrate. However, monolithic arrays present some further optical problems. The most important of these is that the radiation is emitted inside a high refractive index material such as quartz (1) or gallium arsenide (3).

If the radiating dipole is on a parallel slice of material, most of the emitted radiation will be totally internally reflected at the opposite face, producing a trapped surface wave as shown in Fig. 8a. This problem is well known in visible light optics and is usually overcome by placing a thick lens of similar refractive index in contact with the parallel slice. The other surface of the lens is curved so that rays are incident at less than the critical angle. In its simplest form, the centre of curvature of the lens surface lies at the emitting region, so that all radiation meets the lens to air surface at normal incidence as in Fig. 8b. With an array it is obviously impossible to satisfy this condition for every element but in practice departures from the strictly normal incidence condition are used to introduce some refracting

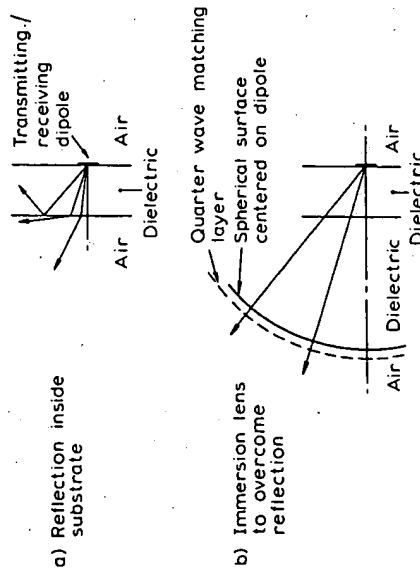


Fig. 8 Imaging through substrate

power and also compensation of optical aberrations produced in other elements of the optical system. With high index materials it is essential to use a good anti-reflection layer (quarter wave matching layer) on the lens surface. Silicon hemispheres could be used with gallium arsenide substrates as the refractive indices of these two materials are almost equal. Alternatively a suitable Stycast material could be used.

As there are only 16 picture elements across the image in our application, it is feasible to place an individual hemisphere over each detector element and use the two element lens designed for open-ended waveguides as shown in Fig. 9. Each hemisphere acts as a field lens, but as they are only about one wavelength in diameter, diffraction effects may overcome the apparent geometrical effect. Hildebrand and Winston (9) have investigated such lenses for low numerical aperture systems, where the lenses are a few wavelengths in diameter. Further theoretical study of the diffraction effects with high numerical aperture systems would appear to be desirable. If this design is feasible, a useful feature is that the active area of the array elements occupies only part of the total substrate slice, leaving room for electrical connections and the other components, resulting in less cross-talk and less dead area. The total size of the substrate slice would, however, be much larger than if a single hemispherical lens is used. This is because the effect of immersion is to decrease the linear size of the geometrical image, and also the diffraction limited spot, by a factor equal to the refractive index of the lens.

A number of lenses have been designed using a single approximately hemispherical silicon lens in contact with an array on GaAs. For good off-axis performance the radius of the hemisphere should be as large as possible, both to reduce field curvature and also to keep the extremes of the array relatively near the axis. A simple two-element lens system for an immersed array with good off-axis performance is shown in Fig. 10a. By careful choice of radius of the hemisphere it is also possible to satisfy the telecentric condition. Some correction for astigmatism has been gained by departing from an exact hemisphere. However the steep radius of the hemisphere introduces appreciable field curvature, and this limits the usable field of view to about $\pm 15^\circ$. It is not possible to correct this with an aspheric surface as we did with the non-immersed lens. A possible

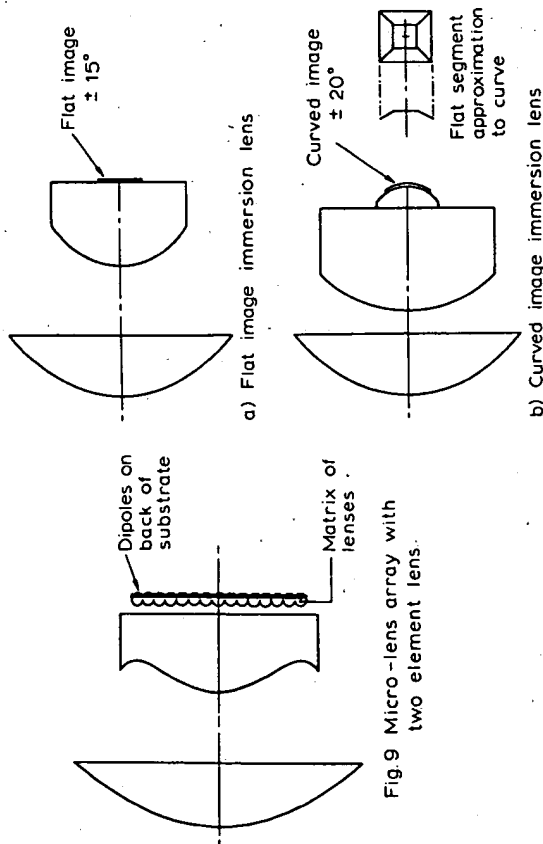


Fig. 9 Micro-lens array with two element lens.

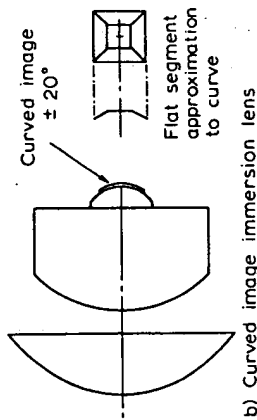


Fig. 10 Lenses for monolithic arrays

solution would be to make the detector array on a curved substrate, but this is ruled out on technical grounds. A compromise is to divide the image into a small number of flat sections as shown at the right of Fig. 10b - three sections for a linear array, or five sections for a two-dimensional array, could cover a field of $\pm 20^\circ$. It is interesting to note that the telecentric condition should not be satisfied for the case of a curved image. The principle ray should meet the curved surface at right angles.

It is possible to design more complicated lenses which give $\pm 20^\circ$ field of view with an immersed image. A negative lens placed in front of any of the lens types described here will increase the angular field of view, but the diameter of such a lens will be greater than the effective on-axis aperture. Such lenses would be very useful where the physical diameter is not limited.

Conclusion

In this paper we have shown that geometrical optics design principles can be applied to millimetre wave lenses with fields of view up to $\pm 20^\circ$, for both open horn arrays and also immersed monolithic arrays. The particular designs described give up to 16 picture elements across the image, thus opening up the possibilities of recognisable pictures at millimetre wavelengths. It now remains to be seen if monolithic technology advances to the stage where a full two-dimensional multi-element array can be realised.

References

- (1) NEIKIRK, D.P., RUTLEDGE, D.B. and MUHA, M.S. Appl. Phys. Lett., 40(3), 1982, p.203-205.
- (2) RUTLEDGE, D.B. and MUHA, M.S. IEEE Trans. Antennas and Propagation, AP-30, 1982, p.535-540.
- (3) BREWITT-TAYLOR, C.R., GUNTON, D.J. and REES, H.D. Electron. Lett., 17(20), 1981, p.729-730.
- (4) DEWEY, R.J. Radio & Elect. Eng., 52, 1982, p.535-542.
- (5) WELFORD, W.T. Aberrations of the symmetrical optical system, 1974, Academic Press, London.
- (6) FRIEDLANDER, F.G. J. Inst. Elect. Eng., 93, IIA, 1946, p.658-662.
- (7) WHITE, W.D. and DE SIZE, L.K. IRE Int. Conv. Rec. Part 1, 1962, p.44-55.
- (8) SIMONIS, G.J. Int. J. Infrared & Millimetre Waves, 3(4), p.439-469.
- (9) HILDEBRAND, R.H. and WINSTON, R. Appl. Optics, 21(10), 1982, p.1844-1846.

Focal Plane Imaging Systems for Millimeter Wavelengths

P. F. Goldsmith, *Fellow, IEEE*, C.-T. Hsieh, *Member, IEEE*, G. R. Huguenin, *Senior Member, IEEE*, J. Kapitzky, and E. L. Moore, *Senior Member, IEEE*

Abstract—We discuss critical aspects of imaging system design and describe several different imaging systems employing focal plane array receivers operating in the 3mm–2mm wavelength range. Recent progress in millimeter-wavelength optics, antennas, receivers and other components permits greatly enhanced system performance in a wide range of applications. We discuss a radiometric camera for all-weather autonomous aircraft landing capability and a high sensitivity cryogenically cooled array for use in radio astronomical spectroscopy. A near-focus system for identification of plastic materials concealed underneath clothing employs a two element lens, and has been demonstrated in active (transmitting) and passive (radiometric) modes. A dual mode imaging system for plasma diagnostics utilizes both active and passive modes at its ≈ 140 GHz operating frequency to study small-scale structure. The radiometric imaging systems employ between 15 and 256 Schottky barrier diode mixers while the imaging receivers for the active systems include 64 element video detector arrays.

I. INTRODUCTION

IMAGING can be considered to be the process of measuring the radiation arriving from different directions. Our experience with imaging derives most directly from our experience with the eye, an optical system employing an array of independent detector elements in the focal surface of an imaging lens. A focal plane imaging array is only one architecture for imaging systems. Obtaining an image of a scene can be carried out in many different ways, several of which are shown schematically in Fig. 1. It is possible to build up an image of a scene by scanning a single pixel receiver, either by moving a detector in the focal plane of an antenna or mechanically or electrically scanning the beam direction of the system. This technique, while slow and cumbersome, has been the only one available at many wavelengths until very recently. Another type of imaging system is the phased array, in which the signals from a number of independent radiating elements can be processed in order to synthesize beams which effectively are sensitive to radiation arriving from different directions. A close relative is the interferometric array widely used in radio astronomy, in which the signals from different antennas are correlated and an image obtained by carrying out an off-line Fourier transformation of the data.

The millimeter wave region has several important advantages in terms of system design, but these very much depend on the precise application. In a general sense, millimeter wavelength propagation is superior to that found in the infrared and visible spectral ranges in poor weather conditions, and is thus preferable for systems that must operate independent of environmental conditions. Millimeter wavelengths clearly offer better angular resolution for a given antenna diameter than do microwaves, and thus have a great potential advantage, particularly for commercial systems which must fit into restricted envelopes. The particular properties of the interaction of millimeter wavelength energy with materials can offer advantages for certain applications, such as remote sensing of trace gases, and this has been used to very great effect recently in studies of the Earth's atmosphere [1].

The millimeter wavelength region of the electromagnetic spectrum is situated between microwave frequencies, in which range coherent signal processing techniques are well developed, and the infrared region, in which incoherent technology has predominated. It is indicative of the position of the technological frontier to compare the lack of imaging arrays at millimeter wavelengths with infrared cameras which already employ focal plane arrays with thousands of elements [2], and highly sophisticated microwave phased array systems [3].

Phased arrays have, however, been limited in their success at millimeter wavelengths due to difficulties designing efficient radiating elements as well as relatively large feed system loss. Interferometers have been restricted to research applications as a consequence of their cost and complexity. Mechanically-scanned systems have been employed for different imaging applications in the millimeter range, but suffer the very major handicaps of expensive, relatively unreliable mechanical systems together with low data rate from the single receiver utilized. Focal plane arrays have to date been little developed due to problems with developing an effective type of feed for coupling between free space and single mode detectors, as well as the significant issues of cost and complexity inherent in systems employing large numbers of pixels.

Extensive work during the last decade or so on overcoming these problems has resulted in much improved feed elements for focal plane imaging systems, and the potential for very low cost individual radiometers to use in large scale focal plane arrays. As a result of these developments, we have adopted focal plane array technology as our design approach for imaging systems in the 2 mm to 3 mm wavelength range. In this paper we indicate some of the design considerations

Manuscript received October 1, 1992; revised April 15, 1993.

P. F. Goldsmith is with Millitech Corporation and the National Astronomy and Ionosphere Center, Cornell University, Ithaca, NY 14853.

C.-T. Hsieh, G. R. Huguenin, J. Kapitzky and E. L. Moore are with Millitech Corporation, P.O. Box 109, South Deerfield, MA 01373.

IEEE Log Number 9211925.

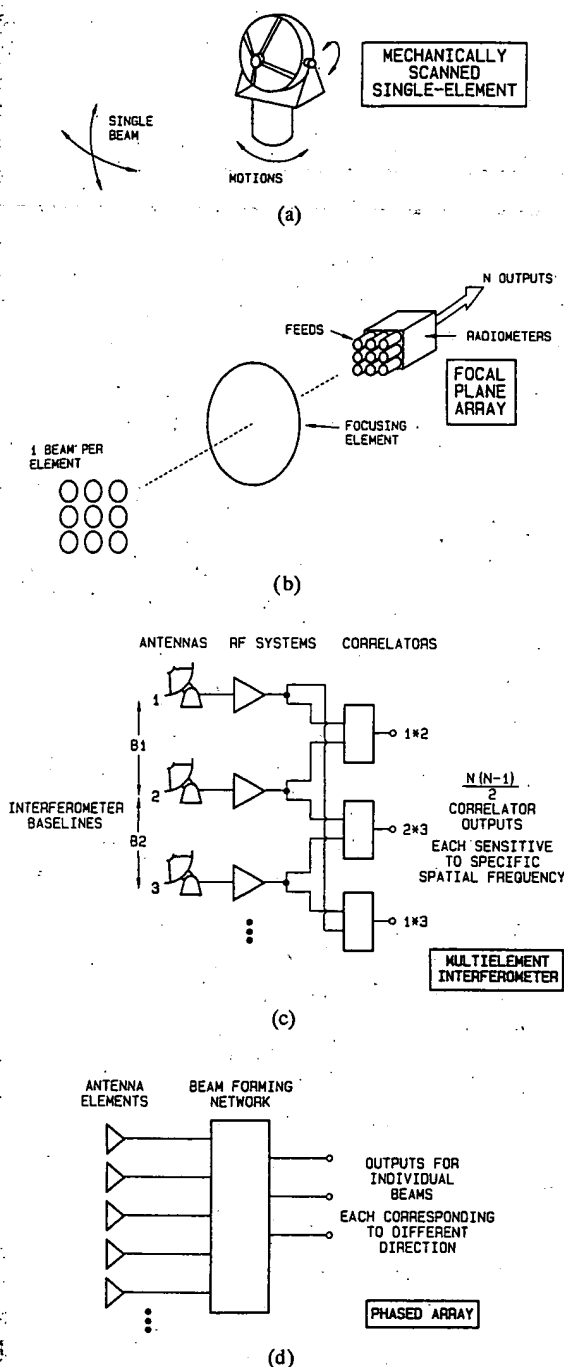


Fig. 1. Schematic of different types of imaging systems (a) mechanically scanned single element; (b) focal plane array; (c) multielement interferometer; (d) phased array.

while its importance for active systems is very much dependent on the configuration. The basic radiometric equation for the rms uncertainty of the scene temperature that can be measured with a coherent detector system (heterodyne or amplifier) is

$$\Delta T_{\text{rms}} = \beta \epsilon T_s / [\delta f \cdot \tau]^{0.5}, \quad (1)$$

where β is a factor, generally between 1 and 2, which depends on the type of radiometer and how the measurement is performed; ϵ is the coupling efficiency between the radiometer and the scene being measured, which includes both antenna-source coupling effects and losses in the input optical system; T_s is the system noise temperature; δf is the predetection bandwidth; and τ is the integration time. All types of systems benefit from efficient coupling and low noise temperature. Systems which are measuring thermal sources can use a relatively large bandwidth to minimize ΔT . Active systems for which the signal is dominated by the return of a transmitted signal are better characterized by their minimum detectable power, given by

$$\Delta P_{\text{rms}} = k T_{\text{rms}} \delta f = \beta \epsilon k T_{\text{rms}} [\delta f / \tau]^{0.5}, \quad (2)$$

where k is Boltzmann's constant. We see that the minimum detectable power increases as the bandwidth is increased, so that in this case, we want the bandwidth to be large enough only to allow the return signal to be processed. If the signal is sufficiently strong, it can be directly detected without any RF processing. In such video detector systems the sensitivity is set by noise fluctuations in the detector element and the predetection bandwidth is generally not a critical parameter.

The sensitivity limits set by the radiometer equation given above, or by video detector sensitivity, are lower limits. A variety of effects can degrade performance, including both instabilities in the radiometer and characteristics of the scene being imaged. Gain instabilities are well known to radiometer designers and can be countered by employing a rapid calibration cycle or switching between the scene and a comparison load (Dicke switching). Single-pixel imaging systems have relied on mechanical scanning of the beam across the scene [4], with calibration performed by looking at thermal loads [5] or by weak coupling of a noise source [6]. For an imaging system with many pixels, a quasioptical input switch is essential for load switching as well as for calibration. The Autonomous Aircraft Landing System discussed below employed a mechanical quasioptical switch, but development of an electronic replacement using PIN diodes has already yielded extremely promising results [7].

In some situations, small-scale variations of the scene temperature which are not of interest set an effective lower limit to the useful sensitivity for studying variations in the scene. As an example, the scenes studied in [6] were characterized by a "clutter" of 2–3 K. With RF/IF bandwidths of several GHz which are now feasible, the noise temperature required to have a radiometric ΔT comparable to or less than this value is quite reasonable, being 10^4 K for $\delta t = 3$ GHz and $\tau = 1/30$ second.

II. GENERAL CONSIDERATIONS FOR IMAGING SYSTEM SENSITIVITY

The relatively low intensity of thermal emission makes sensitivity an important concern for passive radiometric systems,

III. EFFICIENCY, PACKING, AND COST OF ARRAY FEED ELEMENTS

These considerations are central to the successful implementation of any focal plane imaging system and have been discussed in some generality [8], [9], [10]. The feed elements have been the subject of very intense development during recent years. Traditional rectangular horn elements have been compared [11] and developed in monolithic form [12]. A variety of different types of travelling wave slot antennas have been proposed and studied including constant width slots [13] and linearly tapered slots [14]. Other types of feed elements include double dipole [15], Yagi [16] and dielectric rod antennas [17], among others. The general criteria that these designs seek to satisfy include:

- 1) efficient illumination of antenna
- 2) low loss
- 3) effective coupling to active devices
- 4) good packing efficiency.

In addition, qualities such as high polarization purity and reasonable angular divergence end up being of importance in many applications, while low cost is a factor that must be borne in mind particularly for commercial applications.

Achieving good illumination efficiency demands low sidelobes and backlobes, which have been persistent problems for antennas on substrates. This is one of the motivations behind the use of lens-coupled printed circuit antennas, which exploit the tendency to radiate into the dielectric and combine this with collimation of the beam by the dielectric lens [18]. Low loss is an issue with feed elements employing dielectric materials. For commercial systems operating at ambient temperature, the effect is also more severe than for radio astronomical systems in which the feed elements are cooled to low temperature, which greatly reduces their added noise as well as reducing their dielectric loss. Most types of planar designs, including travelling wave slot and dipole antennas, offer good coupling to active devices, either mixers or amplifiers; coupling is, however, a more severe problem for dielectric rod and some other types of antennas.

The question of packing efficiency is an interesting one, as well as being very important for development of effective focal plane arrays. Radio astronomical systems observe essentially non-changing scenes and mosaicking an image by repointing the antenna to fill in points in the focal plane not sampled by the array is, in principle allowed. However, it is generally inefficient to have the array elements too widely separated, since some radio sources will not be very extended compared to the footprint of the array on the sky, and array elements are thus not being used effectively. For commercial applications, where near real-time updating of the radiometric image is required, minimum element spacing is of vital importance to achieve a reasonably well-sampled image without any motion of the antenna.

The ability to sample the image in the focal plane of an antenna is intimately related to proper illumination of the antenna itself by the feed element. We assume that an individual feed is used for each pixel. If it is an aperture-type feed (e.g. horn) then it has a characteristic lateral size to produce the

illumination pattern appropriate to the antenna focal ratio. A close-packed array of such horns cannot fully sample the focal plane because the electric field distribution within the horns is generally quite tapered in order to achieve a radiation pattern with low sidelobes. For scalar feedhorns, for example, close packing of the horns produces only approximately every other beamwidth sampling of the focal plane [10]. Reducing the size of the feed horns results in a broader beam and much reduced antenna efficiency. For travelling wave antennas which derive their gain in part from their length, the situation is more complex, but placing the elements too close together results in interaction via fields and/or currents extending away from the feed elements themselves. In an experimental study, it was found that a 1λ spacing of feeds appropriate for a $f/D = 1$ system was about the minimum that gave acceptable results [17]. Since the distance in the focal plane corresponding to one beamwidth is $\Delta x = f\lambda/D$, this corresponds to about 1 beamwidth spacing.

From a more general viewpoint, full sampling of the focal plane for incoherent illumination of the scene and measurement of the intensity in the focal plane requires an element spacing $\Delta x = 1/2 \cdot (f\lambda/D)$ [19]; in $f/D = 1$ system we thus require an element spacing not much greater than $\lambda/2$. This is far closer to the limiting spacing found theoretically for a variety of feed elements [20]. These authors found that the aperture efficiency for an antenna with slot element feeds, for example, is ≈ 0.5 for $\Delta x \approx 1.15\lambda$ in a $f/D = 1$ system. For a corrugated feedhorn, by contrast, the aperture efficiency has dropped to 0.17 for a spacing just slightly less than this. In the focal plane arrays described below, the constant width slot antennas used with $f/D = 1.1$ optics are generally spaced by 1.35λ , which is about as close as possible without excessive interaction between elements. These systems, while achieving good illumination efficiencies, are clearly far from the desired spacing for full sampling, and from the theoretical limit for reasonable overall system efficiency [21].

IV. IMAGING ABILITY OF FOCUSING SYSTEMS

Analysis of the variation of performance of lens and reflector antennas is a major branch of electromagnetics and has interesting parallels and differences from imaging in optical systems at visible wavelengths. Although work on scanning systems started even earlier, the now classic papers on imaging properties of reflectors [22] and lenses [23] have burgeoned into a literature so vast that it is not possible even to summarize the results, but rather only to give a sampling of references [24].

The issue has, in fact, become rather more acute with recent progress in focal plane array technology—the problem has shifted from one only of academic interest, to a critical aspect of developing practical array systems. The critical parameters include maintaining antenna gain, beam size, and beam quality over the range of angles scanned; achieving these goals is made difficult by a combination of factors including the following:

1) Focal plane arrays with $\approx 10^4$ pixels are being seriously considered, with the result that scan angles ≈ 100 beam widths off boresight must be considered.

2) System aperture diameters are relatively small, typically only a few hundred wavelengths for commercial systems, and often less. Blockage loss for symmetric reflector systems of such limited size is generally excessive.

3) The limited volume available restricts f/D for lens systems to values ≤ 1.25 , which seriously restricts imaging capability. For this same reason, off-axis optical systems are generally not acceptable.

Meeting the requirements in the face of these restrictions is often a very difficult challenge. While it is true that there have been no microwave or millimeter focal plane array systems with number of pixels approaching 10^4 actually implemented, several of the systems discussed below have been designed to be extended to this level, and the imaging properties of the optical systems analyzed accordingly. Imaging lens design studies have primarily been based on analytical treatments, which try to eliminate certain classes of phase error in the aperture plane which are called aberrations. However, the resulting systems are not fully optimized for practical use, given that arrays are modular and the locations of individual feed elements cannot exactly follow a specified focal curve.

Thus it is often necessary to resort to simulations rather than analysis. Full-scale diffraction calculations would be excessively time consuming, so that a hybrid approach that uses Gaussian beam propagation between feeds and optical elements, ray tracing through the lens systems, and finally a single diffraction calculation of propagation to the far-field or to a specified plane where the properties of the beam can be examined is very attractive [25], [26]. With the ever-increasing capability of affordable computers, it should soon be possible to connect this type of imaging analysis program with an optimizing function to obtain best imaging performance over some fixed scan range with appropriate constraints on feed locations. This capability, already available for geometrical optical systems with analysis based purely on ray tracing, should significantly enhance the design capability for diffraction-limited imaging systems.

V. OTHER CONSIDERATIONS

Other considerations in the design of imaging focal plane arrays, which are less fundamental than those discussed above but are nevertheless important, are power dissipation and cost. Even with the current early state of the development of focal plane arrays, it is not too early for these issues to be addressed, especially when extrapolating to larger systems. The basic architecture and geometry of the focal plane array are intimately tied to these questions. For example, while purely planar (e.g. broadside radiating) arrays may be desirable from the point of view of entirely monolithic fabrication, they suffer from problems of inadequate space for complete IF circuits, and potentially from difficulties in thermal dissipation. We have found that the end-

(as discussed below). The full three-dimensional geometry is, in fact, extremely important in making a system which not only can contain the required components, but which can be assembled and serviced effectively.

Power dissipation is already a non-negligible issue for existing arrays. The ambient temperature heterodyne systems discussed below for radiometric imaging consume approximately 200 mW per pixel for the IF amplifiers, or approximately 51 W of power for the 256 element array. Even with the relatively large volume available, dealing with this thermal dissipation is a serious issue. Millimeter wavelength transistor amplifiers are currently undergoing rapid development and are receiving consideration for imaging arrays [27], [28]. These components, while very attractive in terms of low noise performance, are presently problematic in regard to power consumption. A 91–95 GHz amplifier employing 8 stages to achieve the 50 dB gain necessary for direct detection dissipates 560 mW, or almost three times more than the heterodyne system [29]. Clearly, further progress will be required to make RF amplifier systems usable in large-scale integrated arrays and further reduction of power consumption of mixer-based systems is definitely desirable.

Cost is always an issue in systems for commercial applications, but in particular for focal plane arrays with large quantities of millimeter-wavelength circuitry, a small change in the cost per pixel can translate into an impressively large variation in the total cost of a system. Again, technology is changing rapidly, but we have found the use of circuit cards fabricated on "soft" dielectric materials with bonding of discrete and hybrid components to be reliable and cost effective. Radio astronomical and other research-oriented systems with relatively fewer high performing pixels will probably continue to employ waveguide and rigid substrate technology to achieve lowest loss and system noise.

VI. DESCRIPTION OF SOME SPECIFIC SYSTEMS AND RESULTS

In the following we describe a number of millimeter-wavelength imaging systems developed for a variety of applications. Along with basic parameters of the systems, we present some imaging results that have been obtained.

A. 140 GHz Plasma Imaging Camera

Diagnostics of conditions in the ionized gas component of a Tokamak fusion reactor is vital for improving the containment of the plasma and understanding energy loss processes. The camera described in this section was designed to determine from a single "event" or ignition whether small scale fluctuating plasma modes in the interior of the plasma are responsible for plasma transport. Test bed plasma fusion reactors to date have been pulsed systems, with measurements being carried out at a few discrete locations. Although this approach has adequate time resolution, it lacks the spatial resolution necessary to identify the modes which fluctuate over periods of tens to hundreds of microseconds and have scale lengths of centimeters. The configuration and operation of the plasma

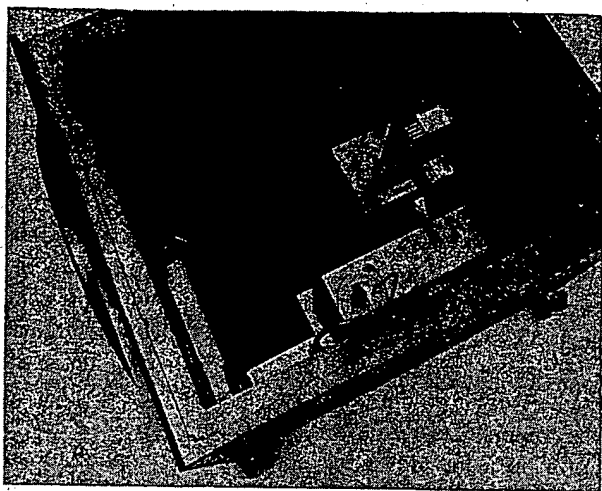


Fig. 2. Photograph of 140 GHz dual mode plasma imaging camera. The transmitter feedhorn is at the lower left, and above it is the 90° reflector to couple its beam to the scene. The focal plane array, local oscillator injection feed, and diplexer, are on the right.

Millimeter wavelength radiation can play several valuable roles in plasma diagnostics. The intensity of emitted radiation allows determination of the plasma temperature, while the reflected signal can yield information about the density structure in the ionized gas [30]. A dual mode plasma imaging camera has been developed for the Princeton Plasma Physics Laboratory to take advantage of both of these capabilities, with an emphasis on studying small-scale fluctuating plasma modes. The imaging system, shown in Fig. 2, includes a 4 by 16 element focal plane array operating at 140 GHz. This frequency is dictated by the properties of the plasma in the Tokamak Fusion Test Reactor.

The feed elements are constant-width slot antennas, and the down converters are second harmonic mixers pumped by a phase locked 70 GHz Gunn oscillator. In its radiometric mode, a 2 GHz bandwidth IF is amplified and detected. For reflectometry, a 30 mW transmitter at approximately 140 GHz illuminates an area of the plasma about 30 cm in diameter. Each beam from the focal plane array is focused by the 1 m diameter lens to an area about 1.5 cm diameter at the plasma, which is approximately 2 m away from the camera. The return signal is processed to obtain in-phase and quadrature signals from which the phase of the reflected signal can be obtained.

B. Detection of Concealed Weapons and Explosives

In recent years the ability to detect plastic weapons and explosives concealed beneath the clothing of airline passengers has received increasing interest by law enforcement and security agencies. To be effective, such detection devices must 1) have a low false alarm rate, 2) be non-invasive, and 3) have high throughput. Both active (reflecting) and passive (radiometric) millimeter wavelength imaging systems have been investigated for these purposes. Frequencies between 30 and 300 GHz provide a number of advantages including 1) low absorption by most dry dielectric materials, 2) moderately high spatial resolution, and 3) good imaging capability via compact optics.

Measurements of a number of materials at 95 GHz (see Table I) have shown that substances such as polycarbonate, polypropylene, rexolite and black delrin have reflectivities in the range -8 to -12 db. The reflectivity of various portions of the human body range from -11 db (calf) to -15 db (jaw). Furthermore, a wide variety of tested clothing items show reflectivities in the range of -15 to -25 db with transmission losses of less than 0.5 db. It appears, then, that dielectric materials of interest have reflectivities 2 to 4 times that of human skin, while clothing provides little in the way of absorption or extended reflectivity.

With imaging spot size being proportional to the product of the imaging lens f/D ratio and the wavelength of operation, it is clear that improved resolution can be obtained by operating at higher frequencies. However, at submillimeter and short millimeter wavelengths, materials are too lossy and the technology for cost-effective imaging systems is not available. At longer (microwave) wavelengths, the technology is well developed but the spatial resolution is inadequate. If the system optics are designed such that f/D is approximately 1, then a wavelength of 3 mm gives a spot size adequate for the recognition of potentially harmful hidden plastic objects. To achieve high throughput of subjects, an array of detectors sampled at video rates (30 Hz) is an attractive approach. The necessary optics must be capable of a large field of view (e.g. ± 30 degrees) with diffraction-limited performance.

Reflective imaging makes use of a relatively intense millimeter wave source to illuminate the subject. Higher reflectivity portions of the subject result in a higher output from the system. An extended array of slot antennas can then produce a video image or a smaller array can be mechanically scanned about the subject (albeit at the cost of reduced throughput). The major problem with this approach is the presence of "glints" in the millimeter wave image due to reflections of illumination sources from boundaries in the subject's clothing. This effect is well known from active millimeter-wave radar imaging of tactical targets [31].

Investigation is proceeding on two approaches to solve this problem: 1) using a number of lower level sources to illuminate the subject from a wide range of angles, and 2) investigating the behavior of a subject rotating in the field of view of the imaging device. It appears that the "glints" are highly dependent on the source-subject-detector geometry and change rapidly as this geometry varies, whereas reflections from real objects have longer duration.

To study the performance of concealed object detection systems, a mannequin was covered with a millimeter wave absorptive material that approximates the absorption characteristics of human skin. The mannequin was then clothed with objects concealed on the torso. A 64 element focal plane array imaging array was used, employing endfire slot antennas each of which was coupled to a detector diode. The illumination source produces levels of radiation well below current safety thresholds. It consists of a number of Gunn oscillators which are frequency-modulated over a few hundred MHz, amplitude-modulated, and also amplitude-modulated. An appropriate synchronous detector circuit at the output of the slot antennas converts the reflected return into a dc voltage. The imaging system

Clothing Item
Flannel Shirt
Polyester Blouse
Wool Suit
Cotton Sweater
Terry Cloth
Cotton Muslin
Synthetic Blouse
Nylon Shell
Corduroy
Cotton Shirt
Cotton Shirt
Electric Material
Polycarbonate
Polypropylene
Rexolite
Ceramic (AT)
Black Delrin
Human Skin Reference

Calf
Forearm
Palm
Back of Hand
Nail
Chest
Average

Average of parts
The Mean and
is measured

consist of a pair
ing together.
imize the field
could be calculated
the distance
radius of (r)
ried out using
ication, and
Refinement
m waist radius
and code distance
the 64 elements
Y position
the main t

computer-controlled
to animation
ended (48 pixels)
ical video analysis
es of a 48 element
image taken
ulation with
es were over
nce a short
a typical ani
time imaging
is quite
ated with the

TABLE I
CLOTHING, MATERIALS, AND HUMAN SKIN MEASUREMENTS

Sample	Thickness (mm)	Reflectivity (dB)	Transmission Loss (dB)
Clothing Item Measured at 95 GHz			
Flannel Shirt	0.5	-18	-0.3
Polyester Blazer	1.2	-15	-1.0
Wool Suit	1.4	-13	-0.8
Cotton Sweater	2.1	-30	-0.7
Terry Cloth	1.0	-22	-0.3
Cotton Muslin	0.5	-13	-0.7
Synthetic Blouse	0.1	-24	-0.04
Nylon Shell	0.1	-23	-0.1
Corduroy	0.6	-16	-0.4
Cotton Shirt (Dry)	0.2	-18	-0.3
Cotton Shirt (Wet)	0.2	-14	-1.0
Electric Material Measured at 95 GHz			
Polycarbonate	5.5	-8.5	-1.8
Polypropylene	1.5	-8.8	-0.8
Rexolite	7.7	-10.7	-1.6
Ceramic (ATD 6)	2.6	-4.5	-3.0
Black Delrin (Front Knurled)	13.0	-12.0	-3.5
Human Skin Reflectivity 90-100 GHz ¹			
		Reflectivity (Mean, Range dB ²)	(Mean, Percent)
Calf		-11.3 ± 1.5	7.4
Forearm		-8.4 ± 2.2	14.5
Palm		-13.4 ± 5.2	4.6
Back of Hand		-11.5 ± 3.3	7.1
Thigh		-15.0	3.2
Average		-11.4 ± 4.4 dB	7.2 Percent

Average of parameters measured over this frequency range

The Mean and Range refer to variation among the 2 to 4 individuals measured except in cases for which no Range is given, where only one individual was measured

ist of a pair of plano-convex lenses with curved surfaces ing together, as shown in Fig. 3. The optics are designed to imize the field of view over which a uniform focused spot could be obtained. The detector-lens distance is 30 cm, the distance between the lens and the focused spot with a radius of 0.55 cm is 60 cm. The initial optics design was ed out using standard Gaussian beam design neglecting ation, and treating the focusing elements as a thin lens Refinement of the design, emphasizing maintaining the waist radius at the subject, was carried out by using d code discussed above [25].

64 element imaging system was integrated with an Y positioner to allow for extended image scanning the main torso of the mannequin. In combination with ounter-controlled video equipment and rotational platform, animations were made to show how the output of an ed (48 pixel by 48 pixel) imaging device might appear. l video animations consisted of 360 individual static r of a 48 cm by 48 cm portion of the mannequin, image taken with the mannequin in a slightly different ation with respect to the camera. These static computer ere overlaid upon the output of a video camera to ce a short video sequence. Fig. 4 shows a still image yptical animation. The results of the study indicated that me imaging of a moving subject to locate hidden plastic is quite effective and greatly reduces the confusion med with the glints seen in static images.

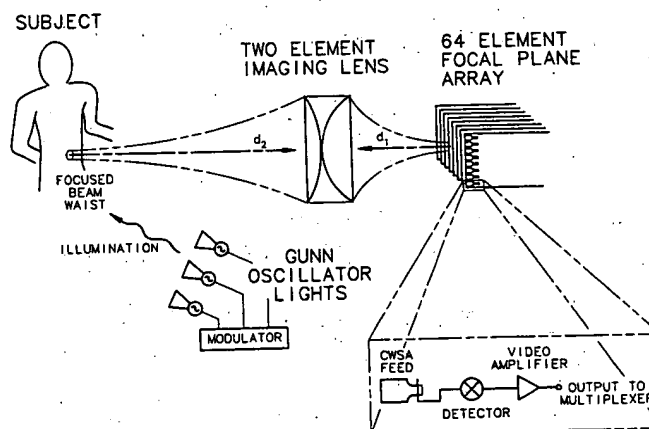


Fig. 3. Schematic diagram of active mode (reflective) contraband detection system.

Radiometric imaging in this context makes use of the thermal emission of the subject and reflected thermal signals from the background. The definition of emissivity, being the complement of reflectivity, implies that a highly reflective target has low emissivity. Thus a radiometric imager sees less of a highly reflective object and more of the background emission. The radiometric detectors receive contributions from the background, the subject and its coverings, and any hidden objects. Reflective objects, having a lower emissivity, would appear cold relative to the body's higher temperature. An

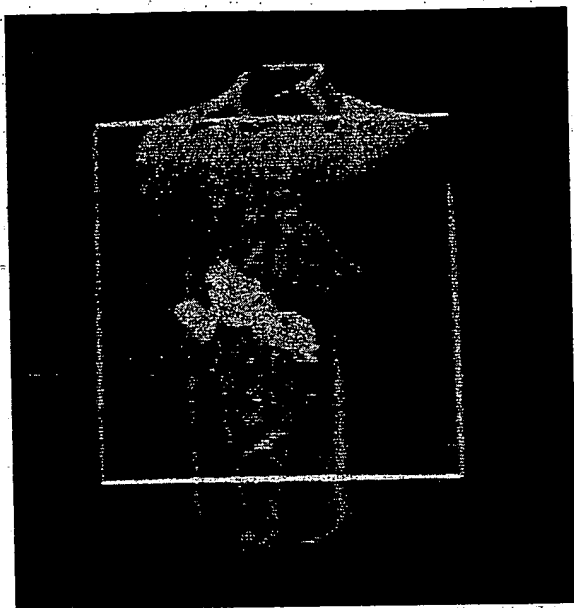


Fig. 4. Image of mannequin with concealed weapon under shirt obtained with active (reflective) imaging system. The 94 GHz image is superimposed on a visual image obtained with a television camera.

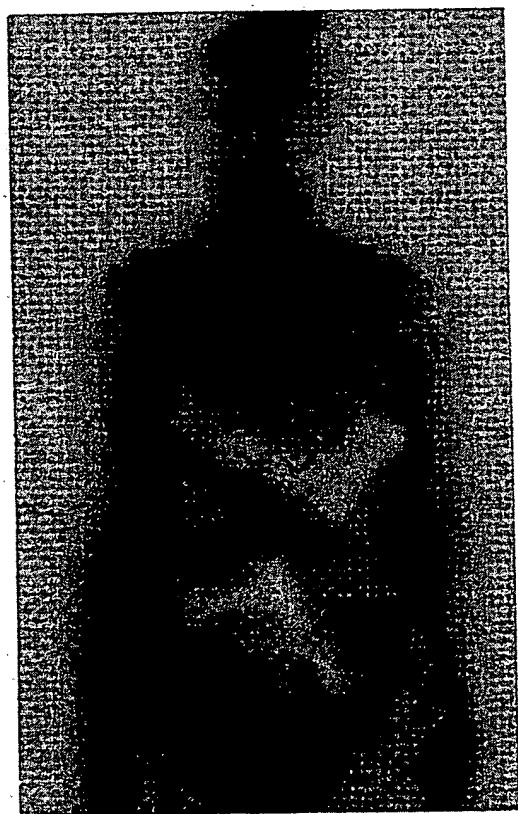


Fig. 5. Radiometric image of male subject carrying concealed weapons under clothing. The upper weapon is a metal gun, while the lower one is a primarily plastic device. Darker areas correspond to regions of increased emission.

example of a radiometric image of a subject carrying two concealed weapons is shown in Fig. 5.

The drawbacks to the radiometric approach are 1) requirement for the high sensitivity necessary to detect natural thermal

emission at millimeter wavelengths, 2) the relatively more complex detector hardware, and 3) the concurrent relatively high cost. However, freedom from glints and the absence of any even low-level "source" illuminating the subject are significant advantages.

In summary, millimeter wave sensing provides an effective method of detecting dielectric objects concealed beneath clothing on human bodies. Imaging using multiple element detector or mixer arrays in the focal plane of the imaging optics can give real-time pictures of objects with a resolution of several millimeters. Both active and passive approaches are successful with the active approach offering lower cost but at the expense of greater signal processing demands.

VII. AUTONOMOUS AIRCRAFT LANDING SYSTEM

Current auto-pilot landing systems have not received widespread popularity because of their high cost, complexity, and limited flexibility. Millimeter focal plane array, or staring array, technology can be applied to develop an autonomous aircraft landing system which provides the pilot with forward-looking millimeter wave vision for landing and takeoff under adverse weather conditions. The system is self-contained and does not need any ground-based supporting facilities. Compared with the active radar scanned images, passive radiometric images are very similar to the visual or IR images due to lack of radar clutter, back scattering or geometrical distortion.

A passive 94 GHz staring image array system, which has been developed to demonstrate the feasibility of this technical approach, is shown in Fig. 6. The array has 64 elements in 8×8 arrangement. The system block diagram is shown in Fig. 7. The 8×8 array offers a field-of-view of 2.9 degrees by 2.9 degrees with a 61 cm diameter Gaussian optics zoned lens which has an angular resolution of less than 0.35 degrees. The far-field spacing of the beams is $\cong 1.05$ FWHM beam width. The Load Comparison and Image Scanning (LCIS) subassembly provides radiometric calibration and over-sampling capability to further enhance the system resolution. The wire grid polarizer assures proper polarization to the LCIS subsystem. The perforated highpass filter is integrated with an EMI shielding enclosure to suppress radiation.

The basic building block for the focal plane arrays is the FPA card, which includes eight radiometer pixel channels. Each pixel channel has an endfire slot antenna, mixer, IF amplifiers, and video processing circuitry. The RF signal (from the scene) and the local oscillator are quasioptically injected to the array by the diplexer. The radiometer pixel noise temperature is 4000 K (DSB) corresponding to a noise figure of 11.6 dB, including the losses of diplexer and highpass filter. Eight such FPA cards are stacked together to make an 8×8 array as shown in Fig. 8.

The 8×8 array can be used as a "subarray" or as the starting point to construct larger arrays. The 8×8 subarray has a physical size of $3.5 \times 3.55 \times 13.0$ cm and power dissipation of 22 watts, of which 13 watts is from the IF amplifiers and the remainder is contributed by the video amplifiers and multiplexer circuits. The focal plane array with this level of power dissipation can be cooled by forced air.

Fig. 6. Millimeter wave 61 cm diameter Gaussian optics enclosure.

LENS

SCENE —

Fig. 7. System block diagram.

Fig. 8. Pixel channel block diagram.

Fig. 9. Pixel channel block diagram.

Fig. 10. Pixel channel block diagram.

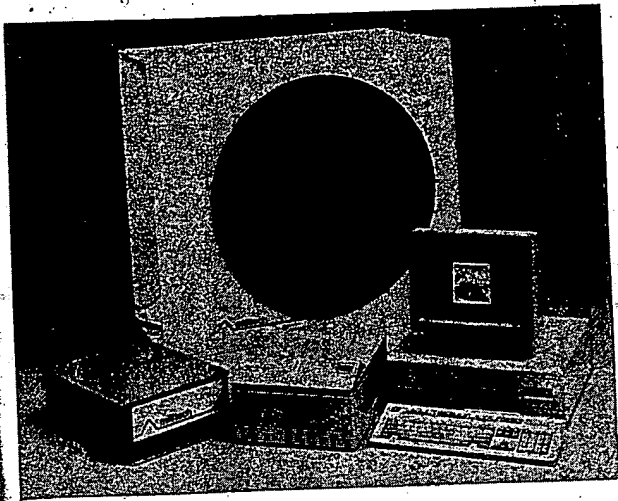


Fig. 6. Millivision™ 64 pixel 94 GHz radiometric imaging system with 30 cm diameter zoned lens. The complete system includes the front-end and optics enclosure, the power supply, and control and display computer.

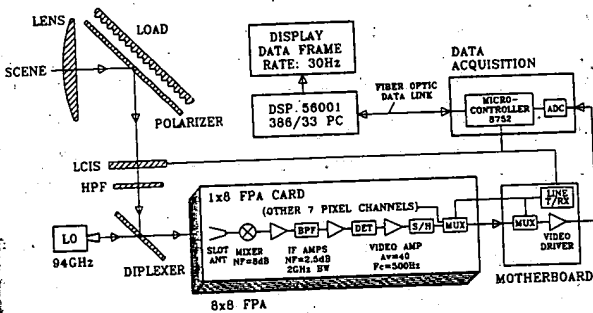


Fig. 7. System block diagram of 8 x 8 pixel 94 GHz focal plane imaging system.

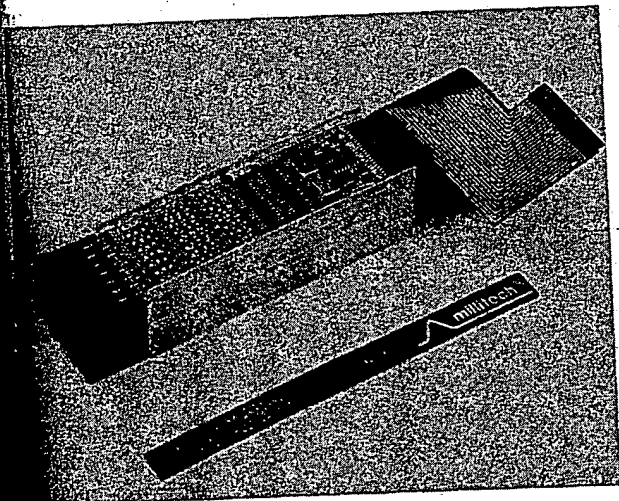


Fig. 8. Photograph of eight cards each with 1 x 8 element array forming a focal plane array. On the top card, the endfire slot antennas are on the top side of the dielectric substrate at the left, the IF amplifiers are in the middle, and the video amplifiers and processing circuitry are on the right.

The modular approach to focal plane array design allows forward extension to larger arrays. A 16 x 16 array as shown in Fig. 9 is based on this approach. Subharmonically-tuned mixers were incorporated in this refined 16 x 16 array.

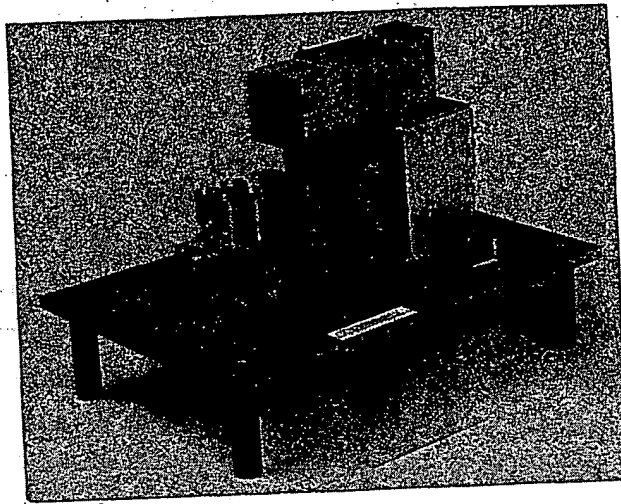


Fig. 9. Photograph of 16 x 16 pixel focal plane array operating at 94 GHz. The four 8 x 8 pixel subarrays can be seen, as can the four local oscillator feed horns, with one L.O. being used to pump the mixers in each subarray. The L.O./signal diplexer has been removed.

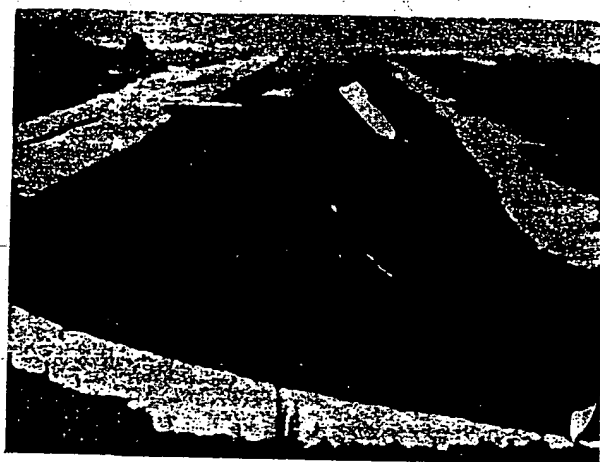
The noise performance of the 16 x 16 array is 5800 K (DSB) or 13.1 dB including the losses of diplexer and highpass filter. In even larger arrays, where the properties of the optical system can easily be configured to conform to the required curved surface.

A comparison between visual, 94 GHz passive scanned images of a scene at the Turner's Falls Airport, Massachusetts, is shown in Fig. 10. Fig. 11 shows a 48 x 48 pixel image which was obtained by stepping the 8 x 8 array in azimuth and elevation. The data update rate from the subarray yielded a new 64 pixel image 30 times per second. The value of image processing, and also the good correspondence with visual imaging, are clearly shown here. Atmospheric attenuation over the few km distance of importance in this application does not result in a significant degradation except during extremely heavy rainfall. With their relatively high data rate, simplicity, and comprehensibility of output, combined with sensitivity and field of view, it is evident that millimeter-wavelength focal plane array imaging systems have major potential for autonomous all-weather landing system applications.

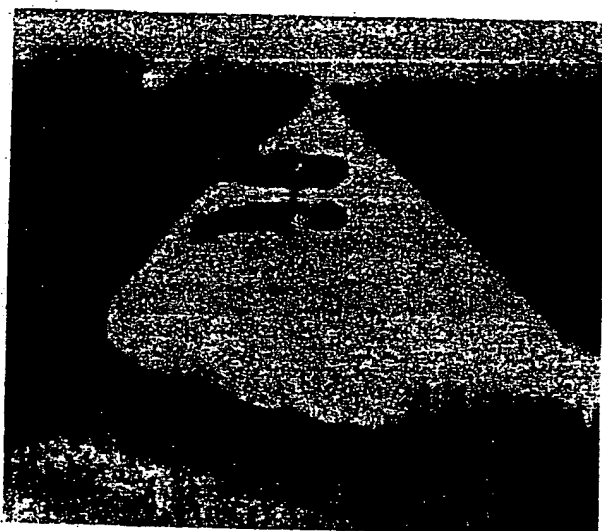
VIII. RADIO ASTRONOMICAL SPECTRAL LINE IMAGING SYSTEM

The most important feature of an imaging system is that it reduces the time required for study of spatially-extended objects, and can allow projects to be undertaken that would be quite unfeasible with a single pixel system. The increase in data rate provided by a multi-element receiver is especially important when the system noise temperature of individual receivers is comparable to the emission from the Earth's atmosphere, because when this point has been reached, further improvements in receiver noise temperature do not yield significant improvements in overall system sensitivity.

This is largely the situation at millimeter wavelengths, due to the appreciable atmospheric opacity (particularly at some astronomically important frequencies such as that of the carbon



(a)



(b)

Fig. 10. Images of runway at Turner's Falls Airport with airplane (a) left hand panel is a visual image; (b) right hand panel is 94 GHz radiometric image. Note that horizon is clearly visible, and that airplane appears "double" due to high reflectivity of runway.

monoxide $J = 1 - 0$ transition at 115.3 GHz), combined with the remarkably low receiver noise temperatures that have been obtained with cooled Schottky [33] and superconducting [34] mixer systems. In some situations, such as studying moderately small sources, the packing density of detector elements in the focal plane is an important consideration and tradeoffs similar to those discussed above must be made in choosing the type of feed element. As discussed in [10], most operational radio astronomical imaging arrays employ scalar feedhorns, but current efforts are to a significant degree focusing on other types of feed elements:

A 15 element focal plane array for astronomical spectroscopy in the 85 to 115 GHz region has already been described in some detail [35], but some of its key features are relevant to the themes developed in this paper. In order to maximize sensitivity, not only the mixers and IF amplifiers are cooled to 20 K, but considerable use is made of cryogenic quasioptical techniques. Thus, the feeds,

48 Pixel by 48 Pixel Image
Taxiway at Turner's Falls Airport (Turner's Falls, Massachusetts,
March 23, 1990)

Unprocessed

Processed



Overlay

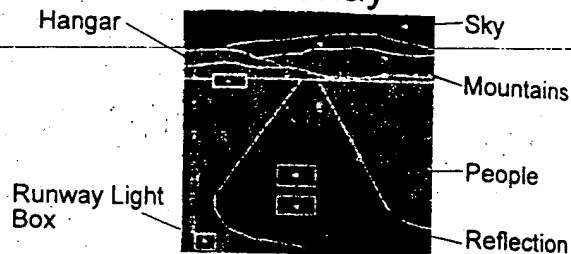


Fig. 11. 94 GHz imaging of scene at airport (a) unprocessed image made from 8×8 mosaic of 64 pixel images with 1 pixel overlap at edges; (b) image processed by median smoothing and histogram equalization; (c) processed image with overlay indicating major visible features.

imaging optics, single sideband filter (a novel design which functions for all 15 beams [36]), and image termination are also cooled. The system uses scalar feedhorns, but with the corrugations removed to form four flat areas which permits a 25% reduction in spacing (including the thickness of the walls and corrugations). The final feedhorn diameter corresponds to a spacing of 2 half-power beamwidths at 105 GHz. To further improve the sampling in the image plane the polarization direction of the beams of the 2×3 subarray are rotated by 90° relative to that of the 3×3 subarray, and then interleaved by means of a wire grid polarization diplexer. The resulting footprint of the array has beams with single beamwidth spacing in one direction by every other beamwidth spacing in the orthogonal direction. The footprint of the array beams on the sky is shown in Fig. 12.

Effective utilization of an astronomical focal plane array requires (as do other array systems) extensive software for dealing with the data in the form of images. In the case of spectral line data, the actual data product is a "data cube" with an image having two spatial and one frequency dimension. Tracing the structure of molecular clouds in the interstellar medium of the Galaxy with such an array is enormously facilitated by using the kinematic information which reflects the relative motion of different parts of these objects. With the 15 element QUARRY array on the Five College Radio Astronomy Observatory 14 m millimeter telescope located in the Quabbin watershed (whence the acronym), the resulting angular resolution is $45''$ at a frequency of 115 GHz. We show in Fig. 13 an image of the Monoceros R2 cloud (distance 2600 light years) obtained by Dr. Taoling Xie, which contains approximately 167,000 spectra. This data is restricted to a narrow velocity range of 0.65 km/s, in which the sharp

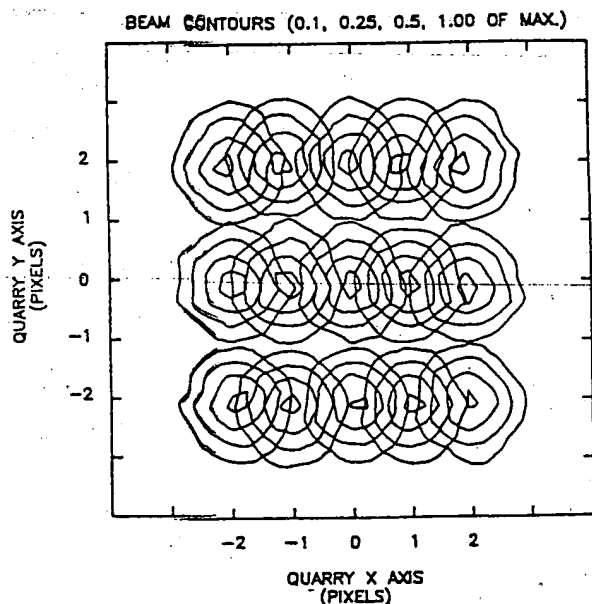


Fig. 12. Contour map of 15 beams from QUARRY focal plane array on FCRAO 14 m telescope measured using Jupiter at a frequency of 110 GHz. The beams overlap at the 0.5 (-3 dB) level in the X direction where polarization interleaving has been employed.

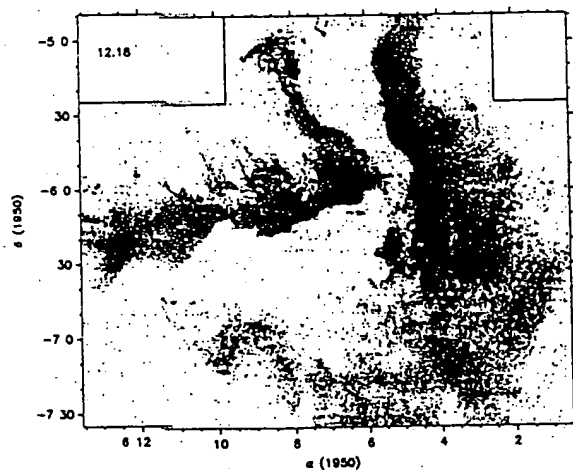


Fig. 13. Map of giant molecular cloud Monoceros R2 made with the QUARRY array system on FCRAO 14 m antenna. The emission is from ^{12}CO in a velocity range 0.65 km/s wide centered on a velocity of the source of 12.18 km/s. The vertical coordinate is declination (degrees and minutes of arc) and the horizontal coordinate is Right Ascension (hours and minutes of time). The entire map covers an area of approximately 2.5 degrees by 3 degrees, while the angular resolution of the telescope is approximately 50".

boundaries of material in the cloud are particularly prominent. These are likely due to shock waves which plausibly are compressing the gas, and thus initiating the formation of new stars. This type of large scale imaging with high angular resolution is essential for unraveling these complex processes and can only be obtained with focal plane imaging systems.

IX. CONCLUSIONS

The unique characteristics of millimeter waves make this

a reasonable cost. As a result of ongoing developments in optics, feed elements, and detectors, millimeter-wavelength focal plane array imaging systems have matured to the point where systems employing tens to hundreds of elements have been developed and used in a wide variety of commercial and research applications. We have described both passive (radiometric) and active (reflected power) systems used for plasma diagnostics, where the frequency allows probing of ionized material in fusion reactors. Millimeter wave radiation propagates through clothing with relatively low loss, and images permit detection of concealed objects including plastic weapons and explosives, offering a valuable tool for airport security. Penetration of weather in conditions of poor visibility allows radiometric imaging of airports and identification of vehicles and other dangerous objects on runways in the context of an autonomous all-weather landing system. Unrivalled sensitivity to emission from molecules at very low temperatures make millimeter-wavelength images enormously valuable for understanding the structure of giant molecular clouds and star formation in the Milky Way Galaxy.

The systems that have been utilized to date undoubtedly represent the first generation of millimeter-wavelength cameras. With further improvements in feed design, it is likely that more complete and efficient sampling of the focal plane will become possible and improvements in sensitivity will result in millimeter-wave images of higher quality having increased fields of view and data rates. This capability will certainly lead to the effective employment of millimeter wave imaging systems in an expanded range of applications.

ACKNOWLEDGMENT

We gratefully acknowledge input regarding plasma measurements from Dr. P. C. Efthimion, and support for the plasma diagnostic camera from the Department of Energy under Contract DE-AC02-88ER80616.002. We thank Dr. Joe Waters for information about atmospheric remote sensing systems. We thank Neil J. McEwan for his contributions to the concealed weapons and explosive system, and for providing research results in advance of publication. Many other individuals at Millitech and at FCRAO devoted considerable time and energy to making these imaging systems possible, and we thank them for their efforts. The field test of the 8×8 demonstration imaging system at Turner Falls Airport, Massachusetts was a joint effort between Millitech Corporation and Applied Technology Division of TRW. The 8×8 demonstration image array system was mainly funded by TRW. The Five College Radio Astronomy Observatory is operated with permission of the Metropolitan District Commission and with support from the National Science Foundation under grant AST91-15721.

REFERENCES

- [1] J. W. Waters, "Microwave limb sounding," ch. 8 in *Atmospheric Sensing by Microwave Radiometry*, M. A. Janssen, Ed. New York: Wiley, 1992.

1674

- [3] See, for example, "Practical Antenna Handbook," by R. Tang in *Antenna Handbook*, R. E. Collin, Ed., New York: Van Nostrand Reinhold, 1988, ch. 18; R. E. Collin, "Antenna array architecture," *Proc. IEEE*, vol. 80, pp. 153-158, 1992.
- [4] J. P. Holm, J. E. Kennedy, and D. Troy, Jr., "A Versatile millimeter-wave imaging system," *IEEE Trans. Microwave Theory Tech.*, vol. MTT-24, pp. 786-793, 1976.
- [5] B. Vainio, J. K. Peltonen, W. Reinert, K. Gruner, and B. Aumiller, "Airborne millimeter-wave imaging system using a cryogenic 90-GHz receiver," *IEEE Trans. Microwave Theory Tech.*, vol. MTT-29, pp. 535-541, 1981.
- [6] W. J. Wilson, R. J. Howard, A. C. Ibbott, G. S. Parks, and W. B. Ricketts, "Millimeter-wave imaging sensor," *IEEE Trans. Microwave Theory Tech.*, vol. MTT-34, pp. 1026-1035, 1986.
- [7] K. D. S. Yngvesson and P. F. Goldsmith, "W-Band quasioptical integrated PIN diode switch," 1992 *IEEE MTT-S Int. Microwave Symp. Dig.*, pp. 591-594.
- [8] D. B. Rutledge, D. P. Neikirk, and D. P. Kasilingam, "Integrated circuit antennas," in *Infrared and Millimeter Waves*, vol. 10, ch. 1, K. Button, Ed., New York: Academic, pp. 1-90, 1983.
- [9] K. S. Yngvesson, "Near-millimeter imaging with integrated planar receptors: General requirements and constraints," in *Infrared and Millimeter Waves*, vol. 10, ch. 2, K. J. Button, Ed., New York: Academic, pp. 91-140, 1983.
- [10] P. F. Goldsmith, "Focal plane arrays for millimeter-wavelength radio astronomy," 1992 *IEEE MTT-S Digest*, pp. 1255-1258.
- [11] E. Li, S. Rengarajan, and Y. Rahmat-Samii, "Comparison between different triangular horn elements for array antenna applications," *IEEE Proc. H*, vol. 138, pp. 281-288, 1991.
- [12] G. M. Rebeiz, D. P. Kasilingam, Y. Guo, P. Stimson, and D. B. Rutledge, "Monolithic millimeter-wave two-dimensional horn imaging arrays," *IEEE Trans. Antennas Propagat.*, vol. AP-38, pp. 1473-1482, 1990; W. Y. Ali-Ahmad, G. M. Rebeiz, H. Dave, and Gordon Chin, "802 GHz integrated horn antennas imaging array," *Int. J. Infrared and Millimeter Waves*, vol. 12, pp. 481-486, 1991.
- [13] Y. S. Kim, and K. S. Yngvesson, "Characteristics of tapered slot antenna feeds and feed arrays," *IEEE Trans. Antennas Propagat.*, vol. 38, pp. 1559-1564, 1990.
- [14] R. Murowin, J. A. Skalar, J. Johansson, and E. Kollberg, "Integrated slot line antenna with SIS mixer for focal plane array imaging applications," *Proc. 17th Eur. Microwave Conf.*, pp. 461-465, 1988.
- [15] D. F. Filipovic, W. Y. Ali-Ahmad, and G. M. Rebeiz, "Millimeter-wave double-dipole antennas for high-gain integrated reflector illumination," *IEEE Trans. Microwave Theory Tech.*, vol. 40, pp. 962-967, 1992; W. Chew, and H. Fetterman, "Millimeter-wave imaging using FET detectors integrated with printed circuit antennas," *Int. J. Infrared and Millimeter Waves*, vol. 10, pp. 565-578, 1989.
- [16] K. A. S. Gassim and J. J. McEwan, "Printed Yagi antennas as a focal plane array in an imaging system," *Proc. 7th Int. Conf. Ant. and Prop. (ICAP'91)*, University of York, U.K., pp. 193-196, 1991.
- [17] K. A. S. Gassim, PhD Thesis, Department of Electrical Engineering, University of Bradford, U.K., ch. 6, 1992.
- [18] K. Uehara, K. Miyashita, K. I. Natsume, K. Hatakeyama, and K. Mizuno, "Lens-coupled imaging arrays for the millimeter- and submillimeter-wave regions," *IEEE Trans. Microwave Theory Tech.*, vol. 40, pp. 806-811, 1992.
- [19] J. F. Johansson, "Millimetre wave imaging theory and experiments," Research Report no. 151, Onsala Space Observatory, Chalmers University of Technology, Gothenburg, Sweden, 1986.
- [20] K. S. Yngvesson, J. F. Johansson, Y. Rahmat-Samii, and Y. S. Kim, "Realizable feed-element patterns and optimum aperture efficiency in multibeam antenna systems," *IEEE Trans. Antennas Propagat.*, vol. 36, pp. 1637-1641, 1988.
- [21] S. Stein, "On cross coupling in multiple-beam antennas," *IRE Trans. Antennas Propagat.*, vol. AP-10, pp. 548-557, 1962.
- [22] J. Ruzic, "Lateral feed displacement in a paraboloid," *IEEE Trans. Antennas Propagat.*, vol. AP-13, pp. 660-665, 1965.
- [23] F. G. Friedlander, "A dielectric-lens aerial for wide-angle beam scanning," *J. Inst. Electrical Eng.*, vol. 93, pt. IIIA, pp. 658-662, 1946.
- [24] C. Dragone, "A first-order treatment of aberrations in cassegrainian and gregorian antennas," *IEEE Trans. Antennas Propagat.*, vol. AP-30, pp. 331-339, 1982; V. Galindo-Israel, W. Veruttipong, R. D. Norrod, and W. A. Imbriale, "Scanning properties of large dual-shaped offset and symmetric reflector antennas," *IEEE Trans. Antennas Propagat.*, vol. 40, pp. 422-432, 1992; ch. 16 "Lens antennas" by J. J. Lee in *Antenna Handbook*, Y. T. Lo and S. W. Lee, Ed., New York: Van Nostrand Reinhold, 1988.
- [25] P. F. Goldsmith, "Perforated plate lens for millimeter quasi-optical systems," *IEEE Trans. Antennas Propagat.*, vol. 39, pp. 834-838, 1991.
- [26] J. Tuovinen, T. M. Hirvonen, and A. V. Raisanen, "Near-field analysis of a thick lens and horn combination: Theory and measurement," *IEEE Trans. Antennas Propagat.*, vol. 40, pp. 613-619, 1992.
- [27] S. Weinreb, "Monolithic integrated circuit imaging radiometers," in *IEEE MTT-S Dig.*, pp. 405-408.
- [28] W. Lam, P. Lee, L. Yujiri, J. Berenz, and J. Pearlman, "Millimeter-wave imaging using preamplified diode detector," *IEEE Microwave Guided Wave Lett.*, vol. 2, pp. 276-277, 1992.
- [29] T. N. Ton, B. Allen, H. Wang, G. S. Dow, E. Barnachea, and J. Berenz, "A W-band, high-gain, low-noise amplifier using PHEMT MMIC," *IEEE Microwave Guided Wave Lett.*, vol. 2, pp. 63-65, 1992.
- [30] Ch. 1, "Instrumentation and techniques for plasma diagnostics: An overview," by N. C. Luhmann Jr., and ch. 2 "Submillimeter interference of high-density plasmas," by D. Veron in *Infrared and Millimeter Waves*, vol. 2, K. Button, Ed., New York: Academic, 1979.
- [31] G. A. Gordon, R. L. Hartman, and P. W. Kruse, "Imaging-mode operation of active mmw systems," *Infrared and Millimeter Waves*, vol. 2, K. J. Button and J. C. Wiltse, Eds., New York: Academic, pp. 327-352, 1981.
- [32] P. F. Goldsmith, ch. 6, "Quasi-optical techniques at millimeter and submillimeter wavelengths," *Infrared and Millimeter Waves*, vol. 2, K. J. Button, Ed., New York: Academic, pp. 277-343, 1982.
- [33] C. R. Predmore, A. V. Raisanen, N. R. Erickson, P. F. Goldsmith, and J. L. Marrero, "A broad-band ultra-low-noise Schottky diode mixer receiver from 80-115 GHz," *IEEE Trans. Microwave Theory Tech.*, vol. MTT-32, pp. 488-507, 1984.
- [34] A. R. Kerr and S.-K. Pan, "Some recent developments in the design of SIS mixers," *Int. J. Infrared Millimeter Waves*, vol. 11, pp. 1169-1187, 1990.
- [35] N. R. Erickson, P. F. Goldsmith, G. Novak, R. M. Grosslein, P. J. Vincuso, R. B. Erickson, and C. R. Predmore, "A 15 element focal plane array for 100 GHz," *IEEE Trans. Microwave Theory Tech.*, vol. 40, pp. 1-11, 1992.
- [36] N. R. Erickson, "A new quasi-optical filter, the reflective polarizing interferometer," *Int. J. Infrared and Millimeter Waves*, vol. 8, pp. 1015-1025, 1987.



Paul F. Goldsmith (M'75-SM'89-F'91) carried out his Ph.D. research developing a sensitive heterodyne receiver for the 1.3 mm wavelength range and used it to make some of the earliest observations of the $J = 2-1$ transition of carbon monoxide and its isotopic variants. This research into the structure of molecular clouds continued at Bell Laboratories, where he was also involved in designing the quasioptical millimeter wave feed system for the 7-m offset Cassegrain antenna.

In 1975 he moved to the University of Massachusetts, Amherst, where he worked on cryogenic mixer receivers and pursued development of quasioptical technology. In 1981 he led a team which carried out the first submillimeter astronomical observations with a laser local oscillator heterodyne system. At the University of Massachusetts, Dr. Goldsmith's astronomical research has addressed questions of the relationship of molecular clouds to young stars and detailed studies of molecular material near the center of the Milky Way. A professor at the University of Massachusetts from 1986 to 1993, Dr. Goldsmith is one of the co-investigators for the Submillimeter Wave Astronomy Satellite (SWAS). In 1993 he joined the faculty of Cornell University as Professor of Astronomy and Director of the National Astronomy and Ionosphere Center. In 1982 he was one of the founders of Millitech Corporation, where until 1992 he was Vice President for Research and Development working primarily in the area of millimeter wavelength imaging and quasioptical component and system design.

Dr. Goldsmith is a member of the American Astronomical Society, Sigma Xi, URSI, and a Fellow of the Institute of Electrical and Electronics Engineers, for which he is also Distinguished Microwave Lecturer for 1992-1993.



Chung-Ta Hsieh received the B.S. in Engineering Science at Cheng-Kung University, Taiwan, in 1970, and M.S.E.E. from Michigan State University in 1975.

He is currently Program Manager, Imaging Systems at Millitech Corporation. He is responsible for coordinating the overall development efforts of the imaging sensor hardware and specific development of the focal plane array. In 1984, he headed the components section for the development of millimeter wave components which included

mixers, multipliers, detectors, switches and filters. He previously worked as Senior GaAs MMIC circuit designer at Texas Instruments in 1988 and was responsible for the development of high speed digital frequency dividers. As Staff Engineer at Hughes Aircraft Company, he headed a NASA 60 GHz integrated receiver project in 1982. He was Senior Engineer at Jet Propulsion Laboratory, California Institute of Technology in 1979 and responsible for the development of analog signal chain for the CCD image system in the Hubble Space Telescope.



John E. Kapitzky received a B.S. in Astronomy from Case Institute of Technology, and M.S. and Ph.D. degrees in Radio Astrophysics from the University of Massachusetts at Amherst.

After graduating, he joined the staff of the Five College Radio Astronomy Observatory as a research engineer, where he helped to develop radio telescope control and data acquisition software. Since 1984, he has worked at Millitech Corporation, where his involvement has been in software design in the areas of data acquisition, imaging, and radar signal processing at millimeter wavelengths. He is a member of the American Astronomical Society and Tau Beta Pi.

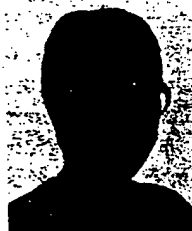


G. Richard Huguenin received the B.S. in Physics from the Massachusetts Institute of Technology in 1959 and the Ph.D. in Astronomy from Harvard University in 1964.

He is currently President and CEO of Millitech Corporation which produces and markets millimeter and submillimeter wave components and systems. From 1963 to 1968 he was on the faculty and directed Harvard's space radio astronomy effort. In 1968, after joining the faculty of the University of Massachusetts at Amherst, Dr. Huguenin established

the Five College Radio Astronomy Observatory, which constructed telescopes and carried out observations at meter wavelengths and in the millimeter frequency range. Under his leadership, the Five College Radio Astronomy Observatory developed into a \$2 million, 60 person organization. He also developed extensive facilities for millimeter and submillimeter instrumentation development.

He has won the Bart Bok Prize from Harvard University, has been a Distinguished Visiting Professor at Chalmers University of Technology, and is a Senior Member of the IEEE with over 40 solely authored scientific and technical articles.



Ellen L. Moore received a B.A. in Physics from Mount Holyoke College, her M.S. in Astronomy, and M.S.E.C.E. from the University of Massachusetts at Amherst.

After graduating she joined the Raytheon Research Division where she contributed to GaAs monolithic circuit design and millimeter wave IMPATT diode testing. Since 1983 she has been in Millitech Corporation, where she has been responsible for millimeter wave antenna and quasi-optics development. This work includes the design and

testing of the optics for imaging systems to be used for all-weather landing systems, plasma diagnostics, automobile and weather radars, and remote sensing systems. She has been the principal investigator on three SBIR programs through Phase 2. Ms. Moore is a Senior Member of IEEE.